Theory and practice of *ab initio* materials design

In-Ho Lee
Materials Genome Center, Korea Research Institute of Standards and Science, Daejeon 305-340, Korea

Collaborators:

Y. J. Oh, S. Kim, K. J. Chang (KAIST)
J. Lee (KIAS)

The 7th KIAS CAC Summer School
KIAS, June 28, 2016

KRISS

The understanding of processing–structure–properties relationships is called the materials paradigm.

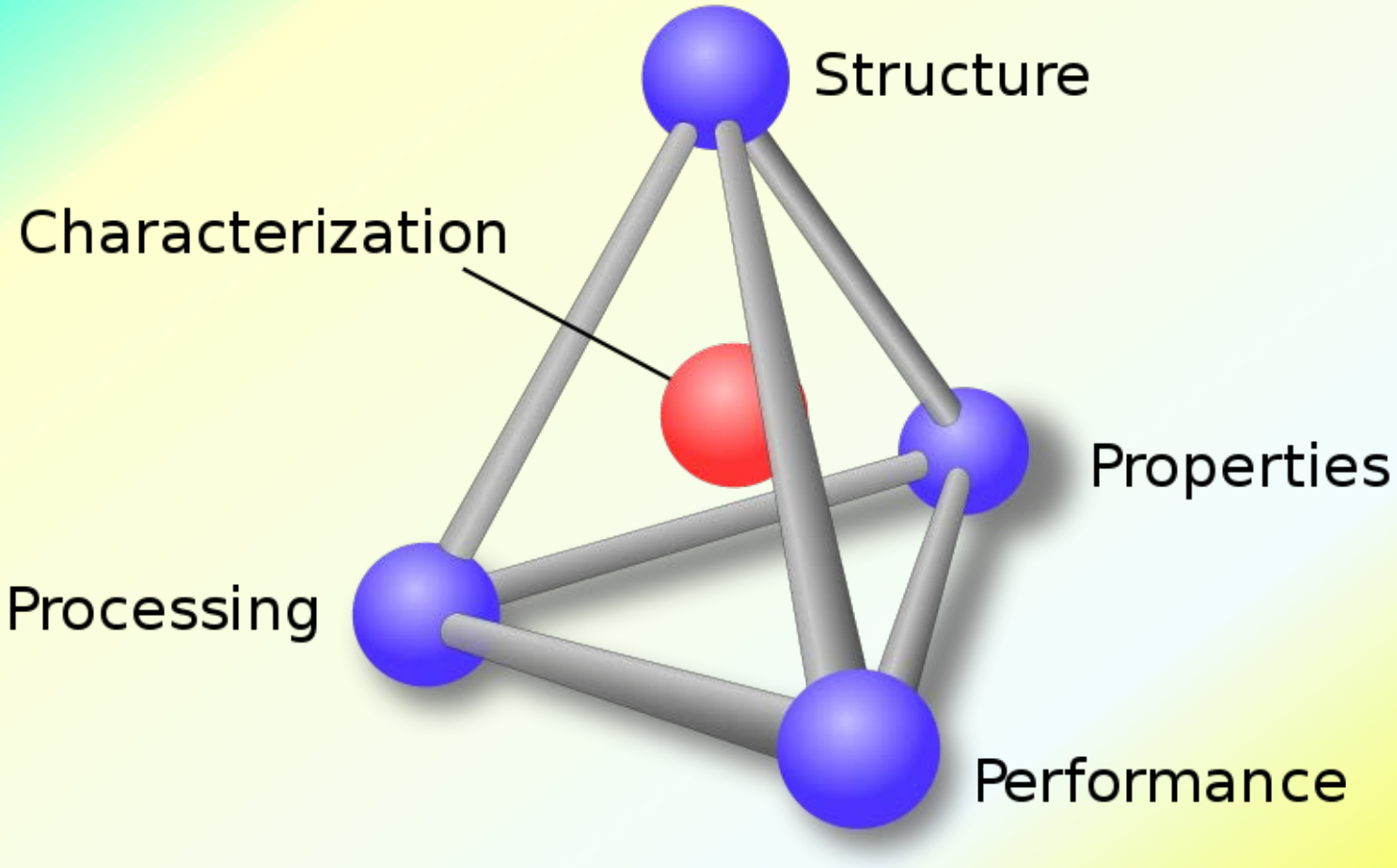

https://en.wikipedia.org/wiki/Materials_science

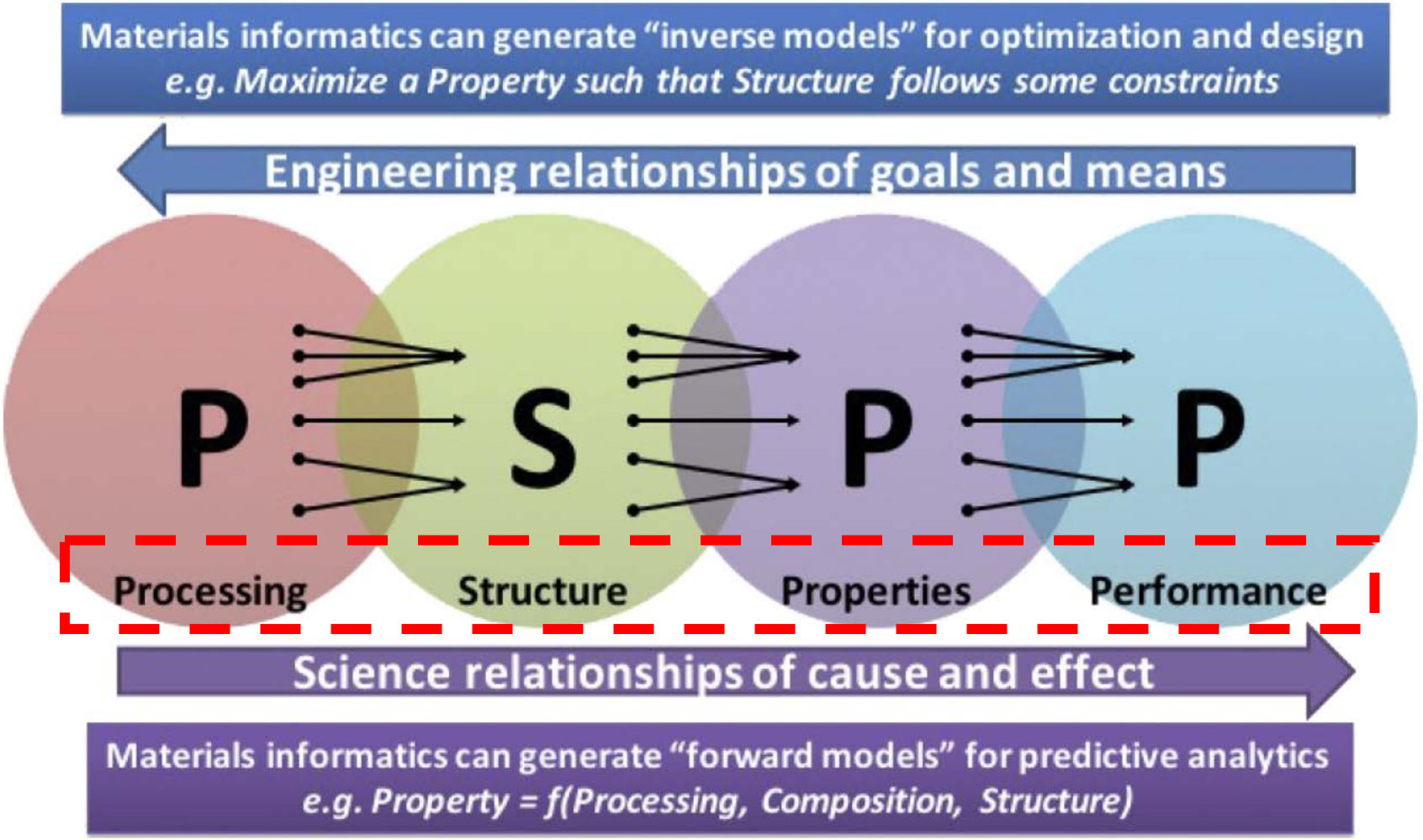

f^{-1}(Property) = {Processing, Composition, Structure},
f^{-1}(Performance) = {Processing, Structure},
f^{-1}(Performance) = {Structure}.

APL Mater. **4**, 053208 (2016).

The inverse band-structure problem of finding an atomic configuration with given electronic properties

$$\text{Atomic configuration} \longrightarrow \text{Electronic structure} \qquad (1)$$

$$\text{Electronic structure} \longrightarrow \text{Atomic configuration} \qquad (2)$$

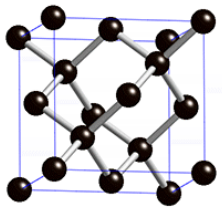

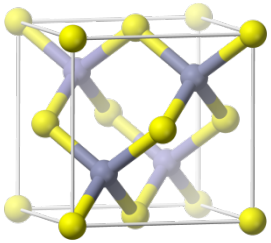

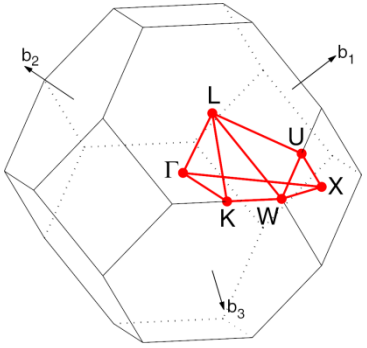

FCC path: Γ-X-W-K-Γ-L-U-W-L-K|U-X

[Setyawan & Curtarolo, DOI: 10.1016/j.commatsci.2010.05.010]

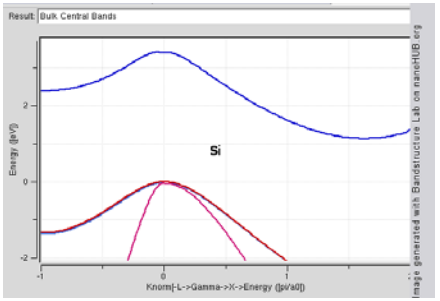

http://en.wikipedia.org/wiki/File:Sphalerite-unit-cell-depth-fade-3D-balls.png
http://en.wikipedia.org/wiki/Brillouin_zone
Nature **402**, 60 (1999).

KRISS

Direct/indirect band gap

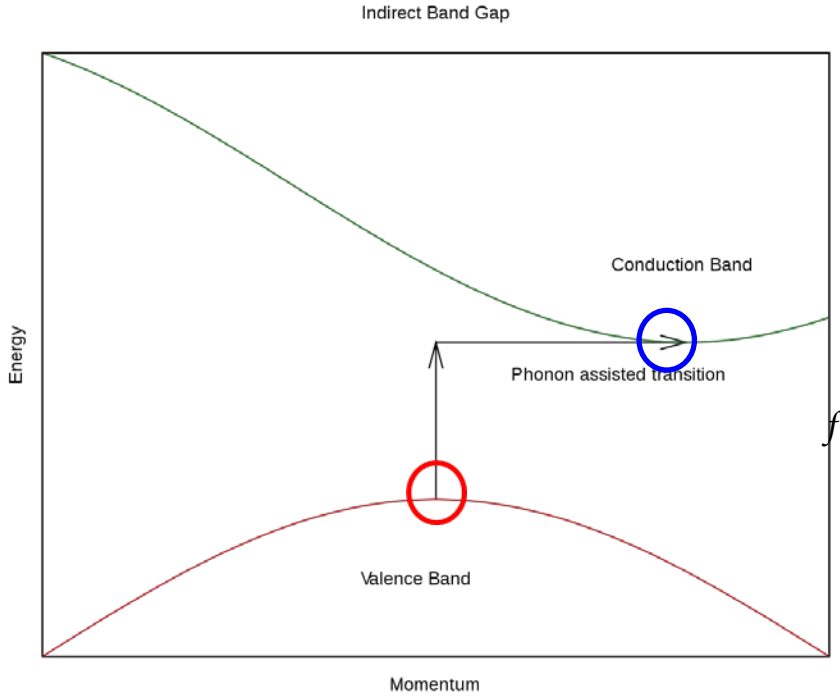

$f p i_2$

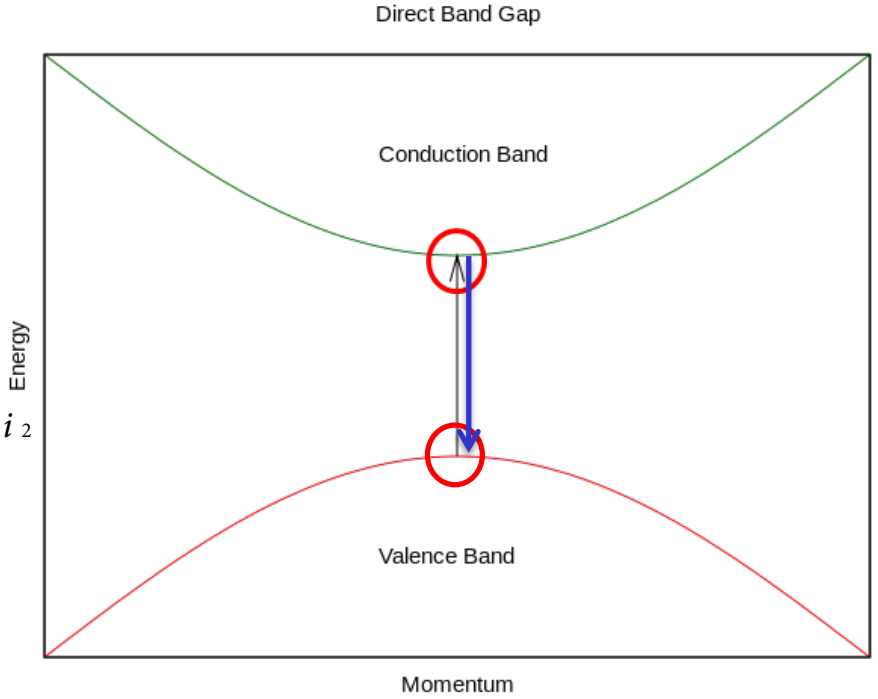

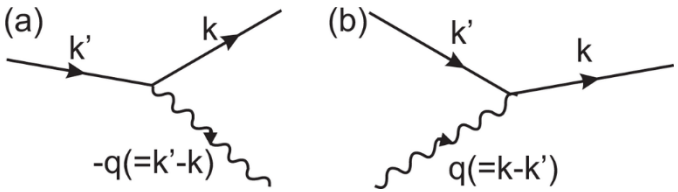

Momentum conservation

$$|\langle f|\vec{p}|i\rangle|^2$$

Dipole-allowedness

https://en.wikipedia.org/wiki/Direct_and_indirect_band_gaps

KRISS


tab
Q
W
S
A
Z
X
D
alt

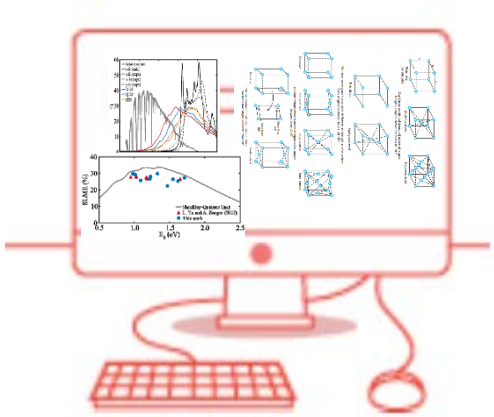

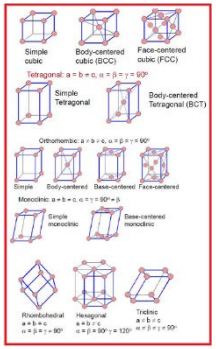
Simple cubic
Body-centered cubic (BCC)
Face-centered cubic (FCC)
Tetragonal: a = b ≠ c, α = β = γ = 90°
Simple Tetragonal
Body-centered Tetragonal (BCT)
Orthorhombic: a ≠ b ≠ c, α = β = γ = 90°
Simple
Body-centered
Base-centered
Face-centered
Monoclinic: a = b ≠ c, α = γ = 90° ≠ β
Simple monoclinic
Base-centered monoclinic
Rhombohedral a = b = c α = β = γ = 90°
Hexagonal a = b ≠ c α = β = 90°, γ = 120°
Triclinic a ≠ b ≠ c α ≠ β ≠ γ ≠ 90°

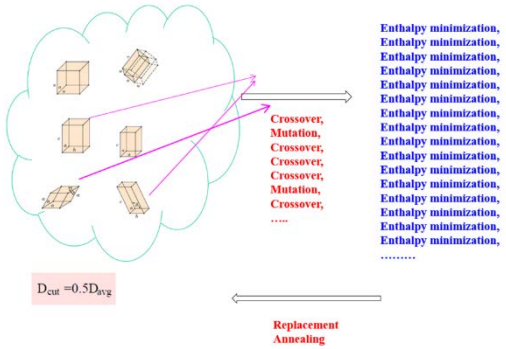
Crossover,
Mutation,
Crossover,
Crossover,
Crossover,
Mutation,
Crossover,
.....
Enthalpy minimization,
Enthalpy minimization,
Enthalpy minimization,
Enthalpy minimization,
Enthalpy minimization,
Enthalpy minimization,
Enthalpy minimization,
Enthalpy minimization,
Enthalpy minimization,
Enthalpy minimization,
Enthalpy minimization,
Enthalpy minimization,
Enthalpy minimization,
Enthalpy minimization,
Enthalpy minimization,
Enthalpy minimization,
Enthalpy minimization,
Enthalpy minimization,
.....
D_{cut} =0.5D_{avg}
Replacement
Annealing

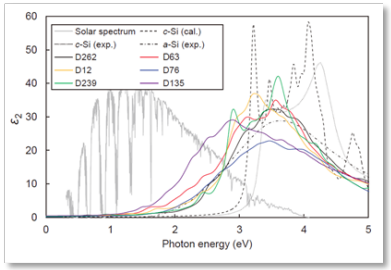
Solar spectrum
c-Si (cal.)
c-Si (exp.)
a-Si (exp.)
D262
D63
D12
D76
D239
D135
ε_2
Photon energy (eV)

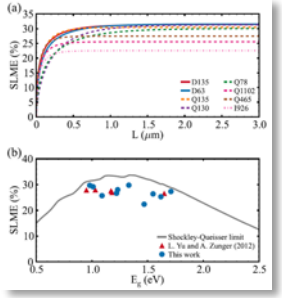
(a)
SLME (%)
D135
D63
Q135
Q130
Q78
Q1102
Q465
I926
L (μm)
(b)
SLME (%)
Shockley-Queisser limit
L. Yu and A. Zunger (2012)
This work
E_g (eV)

KRISS

att532

Padberg and Rinaldi (1987) found the optimal tour of 532 AT&T switch locations in the USA.

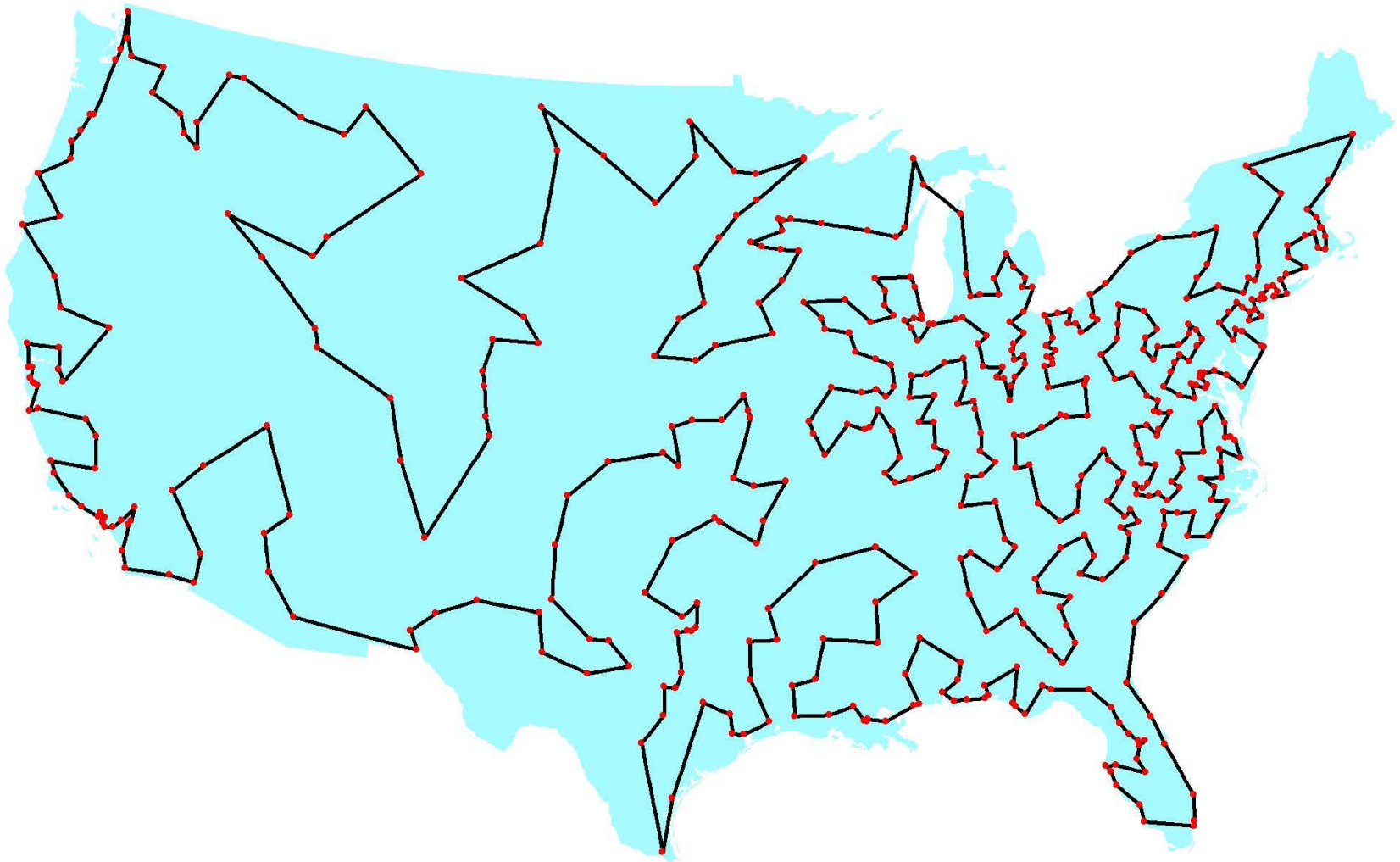

Phys. Rev. Lett. **91**, 080201 (2003).

KRISS

$$V(r) = 4\epsilon\left[\left(\frac{\sigma}{r}\right)^{12} - \left(\frac{\sigma}{r}\right)^{6}\right]$$

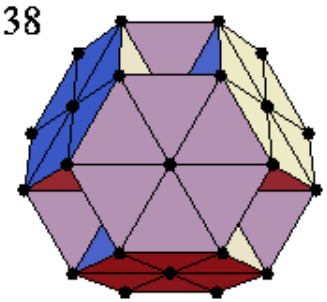

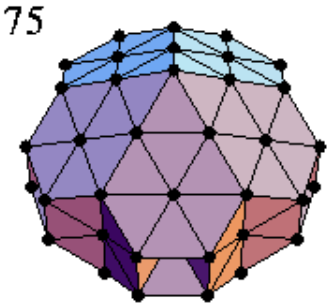

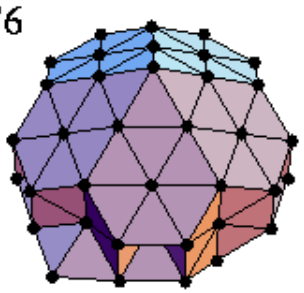

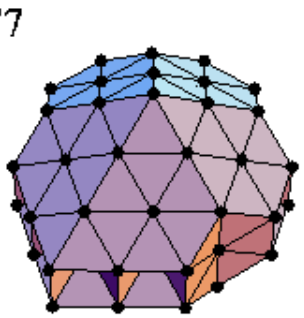

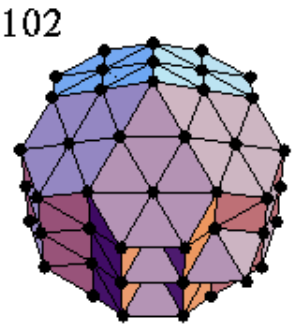

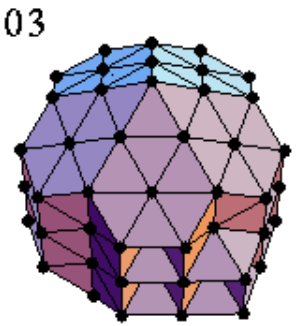

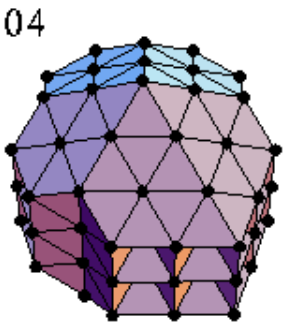

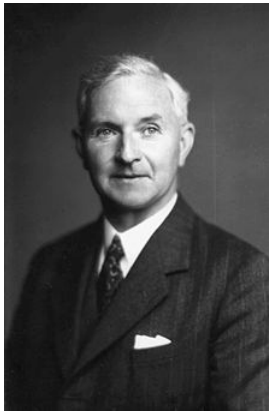

John Edward Jones married Kathleen Lennard in 1926, adding his new wife's surname to his own to become Lennard-Jones.

[John Lennard-Jones]

http://physchem.ox.ac.uk/~doye/jon/structures/LJ/tables.150.html

KRISS

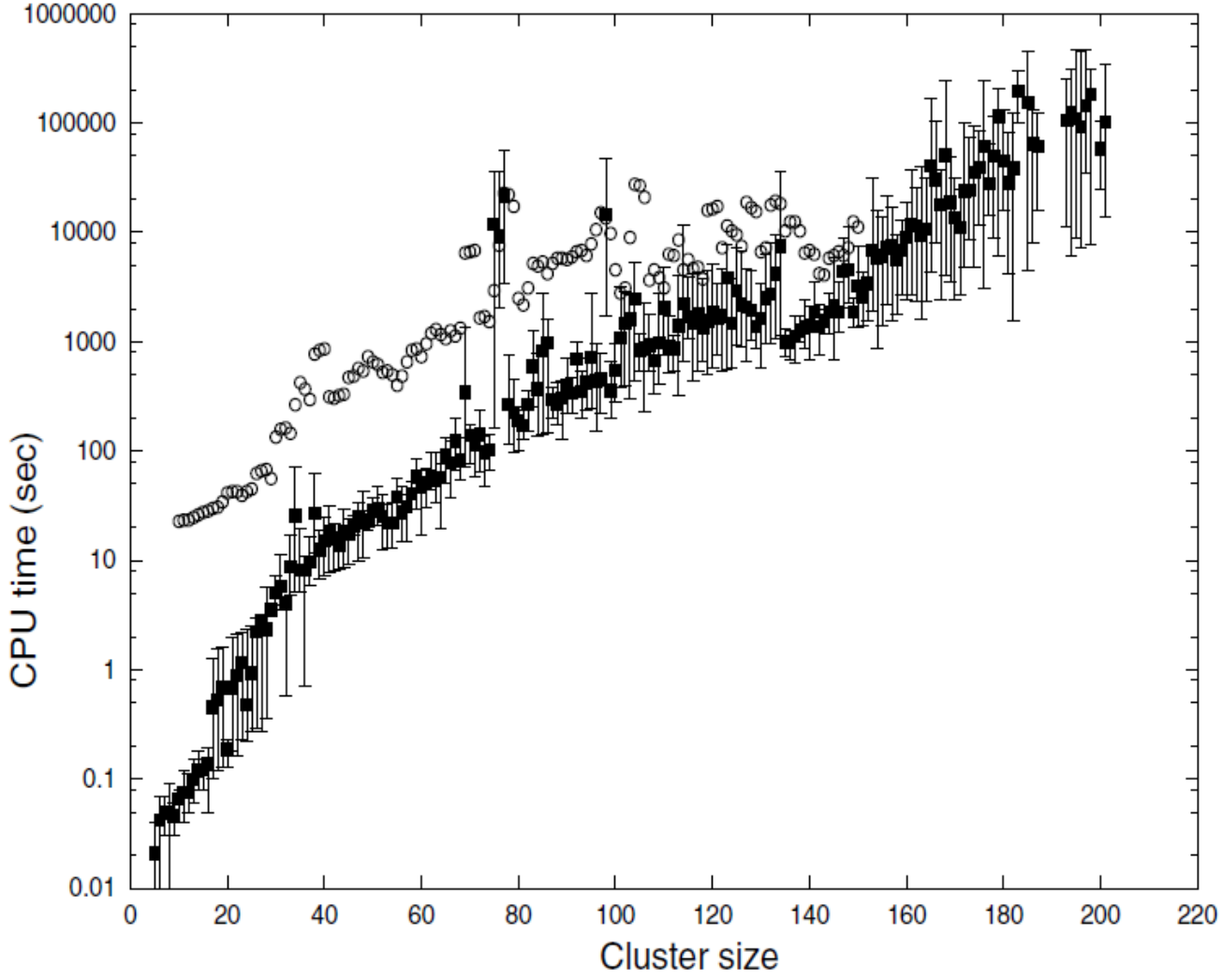

Phys. Rev. Lett. **91**, 080201 (2003).

KRISS

Conformational Space Annealing (CSA)

- Based on genetic algorithm(GA) → maintain a pool of conformations (bank) and new conformations are obtained by mating (crossover) and mutation (small perturbation)
- Consider only conformational space of local minima (as in MCM)
- Diversity of the bank is directly controlled by introducing the concept of distance between the conformations
- Narrows the search to smaller region while maintaining diversity of sampling
- Key idea : GA + annealing in conformational space

Comput. Phys. Commun. **203**, 110 (2016).
Phys. Rev. Lett. **91**, 080201 (2003).
J. Comput. Chem. **18**, 1222 (1997).

Conformational Space Annealing (CSA)

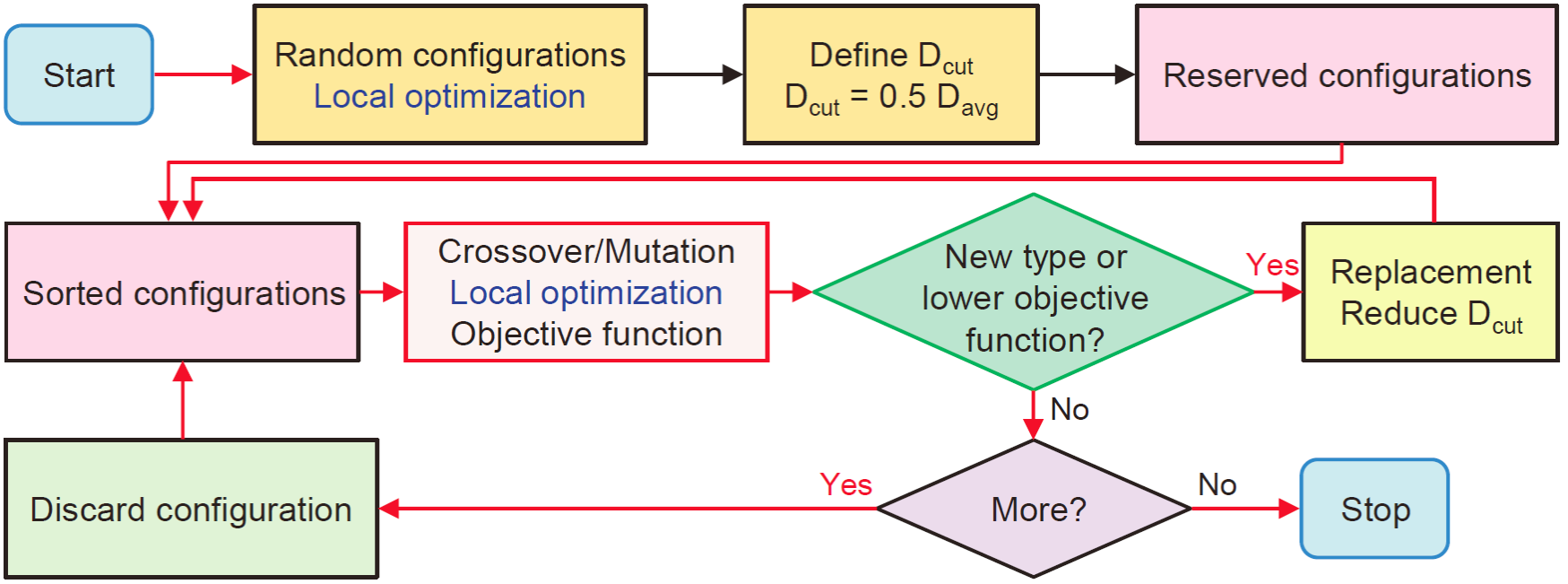

No human intervention

Comput. Phys. Commun. **203**, 110 (2016).

Phys. Rev. Lett. **91**, 080201 (2003).

J. Comput. Chem. **18**, 1222 (1997).

KRISS

Ab initio materials design using conformational space annealing (AMADEUS)

Atomic configuration ⟶ Electronic structure (1)

Electronic structure ⟶ Atomic configuration (2)

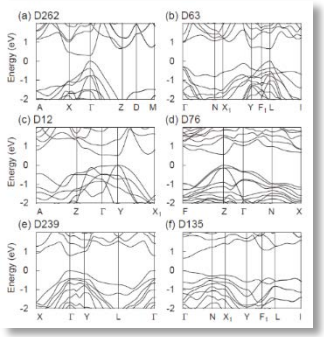

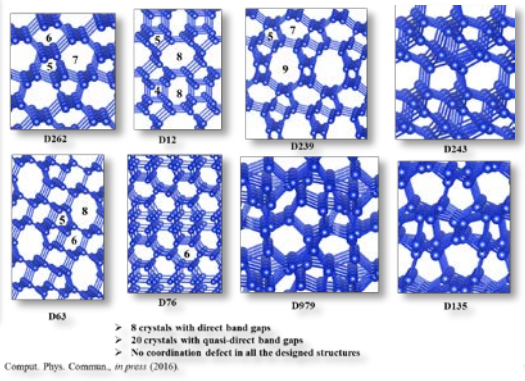

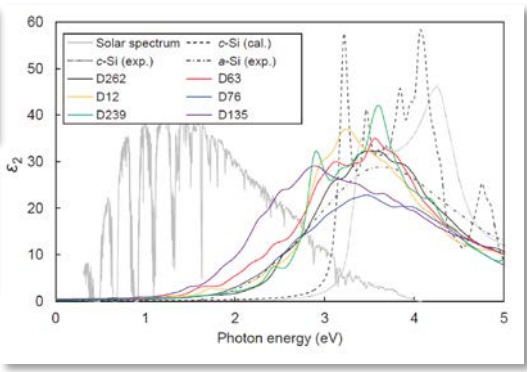

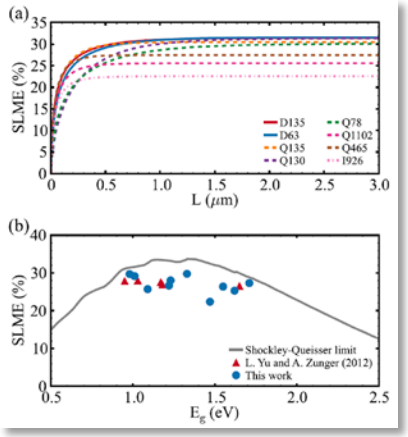

DFT ⟷ Conformational Space Annealing ⟷ Crystal structures ⟷ *GW*-BSE ⟷ SLME

Crystal structures ⟷ Lattice dynamics, Molecular dynamics

Nature **402**, 60 (1999).
Phys. Rev. B **90**, 115209 (2014).
Sci. Rep. **5**, 18086 (2015).

Comput. Phys. Commun. **203**, 110 (2016).

KRISS

Lattice parameters: a, b, c, α, β, γ

230 space groups

14

The 7 lattice systems	The 14 Bravais lattices			
Triclinic	P $\alpha, \beta, \gamma \neq 90°$			
Monoclinic	P $\beta \neq 90°$ $\alpha, \gamma = 90°$	C $\beta \neq 90°$ $\alpha, \gamma = 90°$		
Orthorhombic	P $a \neq b \neq c$	C $a \neq b \neq c$	I $a \neq b \neq c$	F $a \neq b \neq c$
Tetragonal	P $a \neq c$	I $a \neq c$		
Rhombohedral	P $\alpha=\beta=\gamma \neq 90°$			
Hexagonal	P			
Cubic	P (pcc)	I (bcc)	F (fcc)	

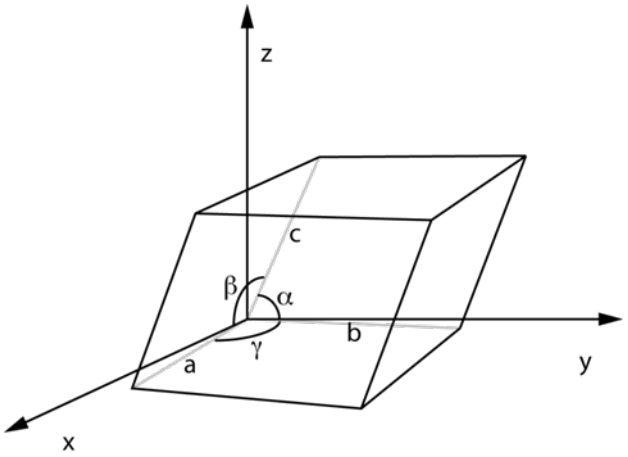

17 space groups

5

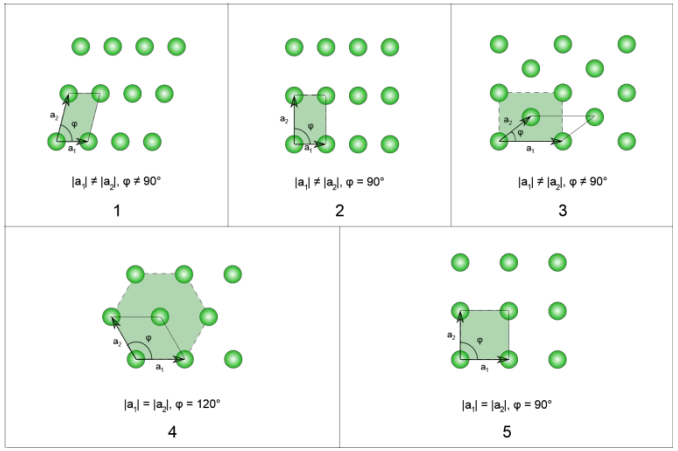

http://en.wikipedia.org/wiki/Bravais_lattice

KRISS

Stable crystals

- The crystal structure must be stable against the local variations of lattice parameters and atomic positions.
- This property must be studied before the investigation of the electronic structure.
- The combined force and stress theorems completely determine the equation of state of the crystal.

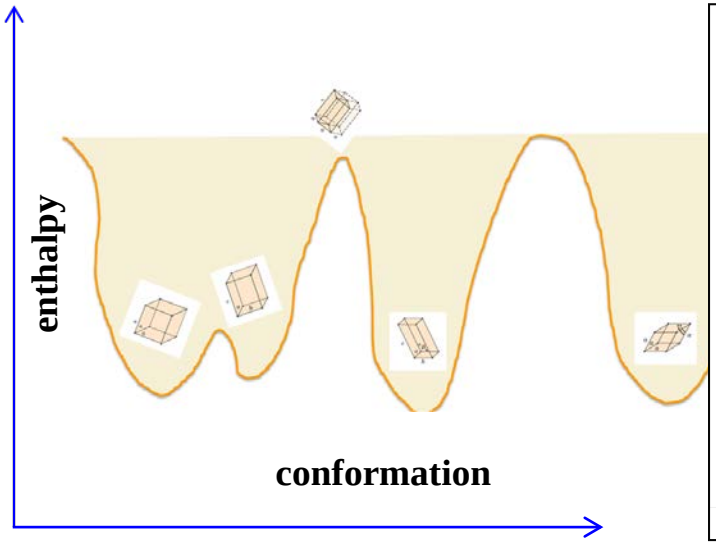

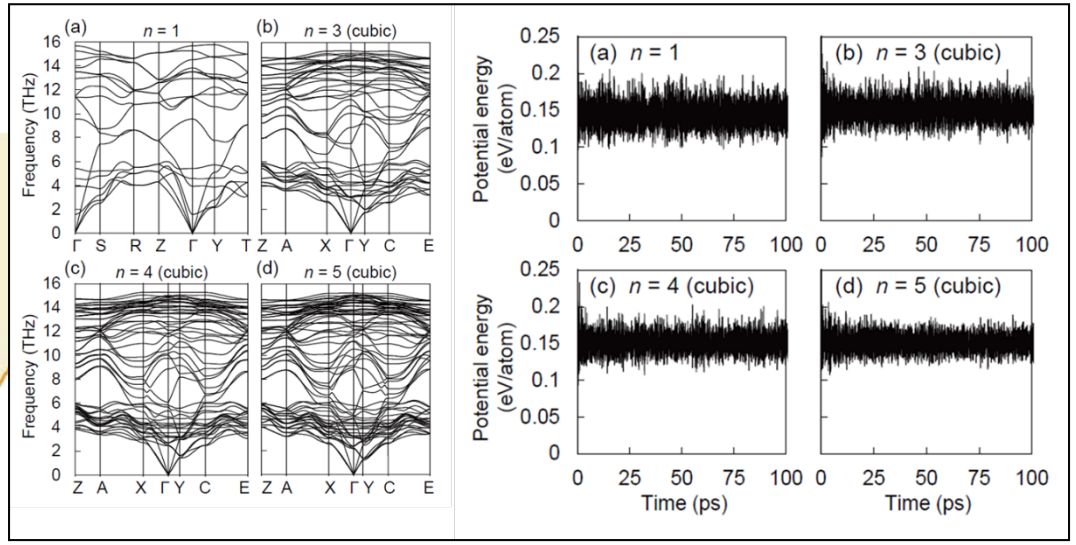

Comput. Phys. Commun. **203**, 110 (2016).

KRISS

Random lattice parameters

- The initial cell is generated by choosing random unit cell translation vectors and renormalizing its volume to lie within a reasonable range.
- It is the most unbiased algorithm that we can think of.
- Bond length : 0.75 ~ 3.0 Å
- cell lengths *(a, b, c)* > 1.2 Å and angles *(α, β, γ)* within 20 ~ 160 degree

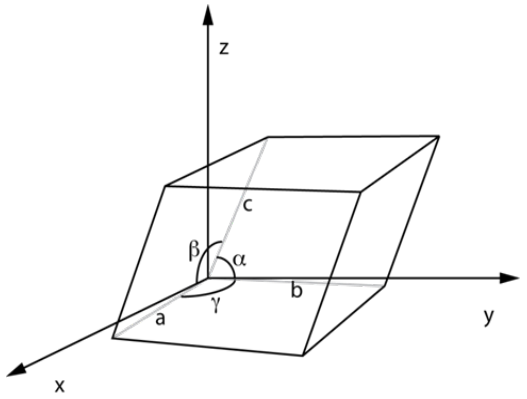

$\Delta k = 2\pi \times 0.12$ Å^{-1}

$\Delta k = 2\pi \times 0.06$ Å^{-1}

$\Delta k = 2\pi \times 0.02$ Å^{-1}

$$20^\circ \le \alpha \le 160^\circ,\ 20^\circ \le \beta \le 160^\circ,\ 20^\circ \le \gamma \le 160^\circ,$$

$$a > 1.2\ \text{Å},\ b > 1.2\ \text{Å},\ c > 1.2\ \text{Å},$$

$$0.3 \le a/b \le 6.0,\ 0.3 \le b/c \le 6.0,\ 0.3 \le c/a \le 6.0.$$

Comput. Phys. Commun. **203**, 110 (2016).

KRISS

Symmetric random structures

- Trial space group→ trial structure
- General/Special Wyckoff positions
- A fully random initialization ←→
- Introduction of symmetric structures
- Good fragments (good structure)

230 space groups

Comput. Phys. Comm. **184**, 1172 (2013).

KRISS

“Parallel in parallel”

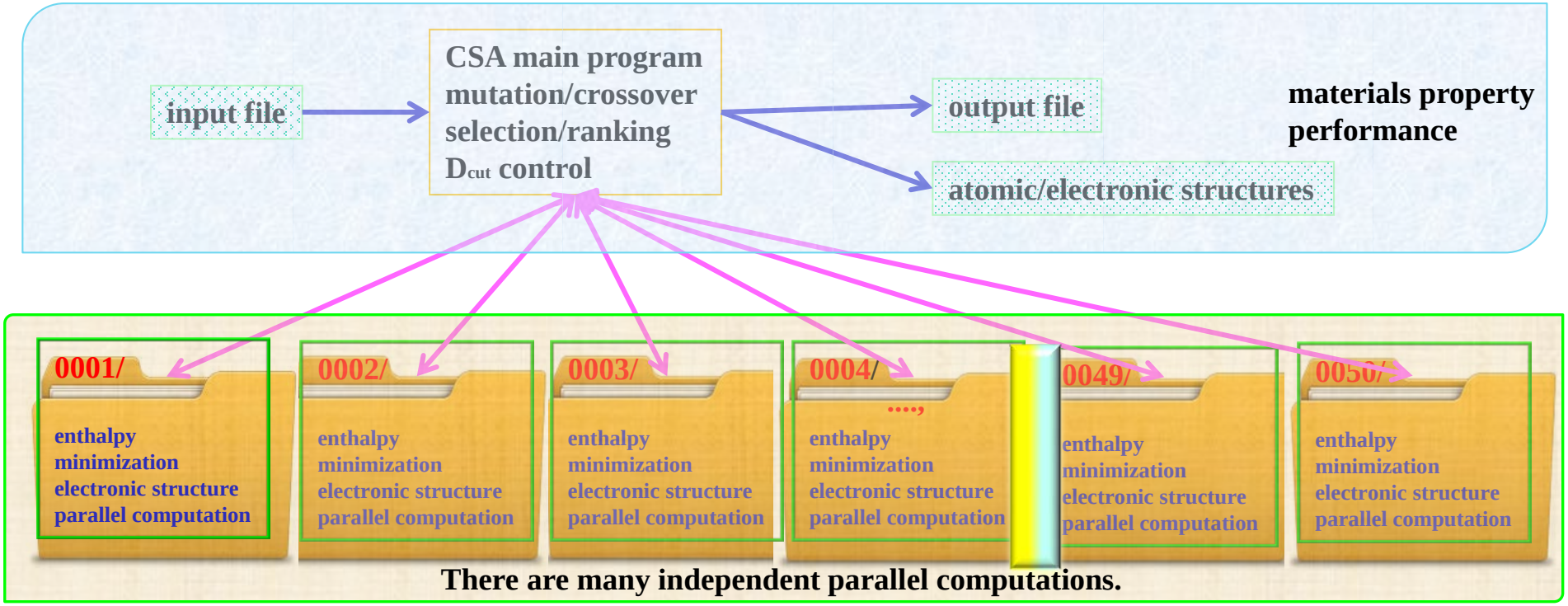

First-principles DFT calculation : many CPUs

InfiniBand
Tightly coupled CPUs

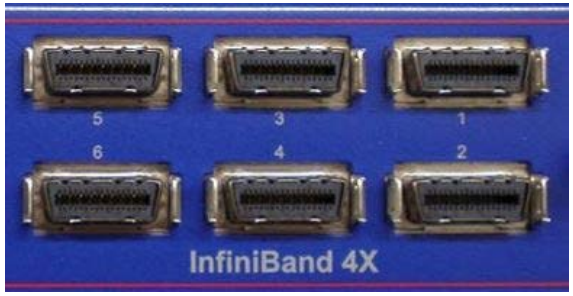

Comput. Phys. Commun. **203**, 110 (2016).

KRISS

“Parallel in parallel”

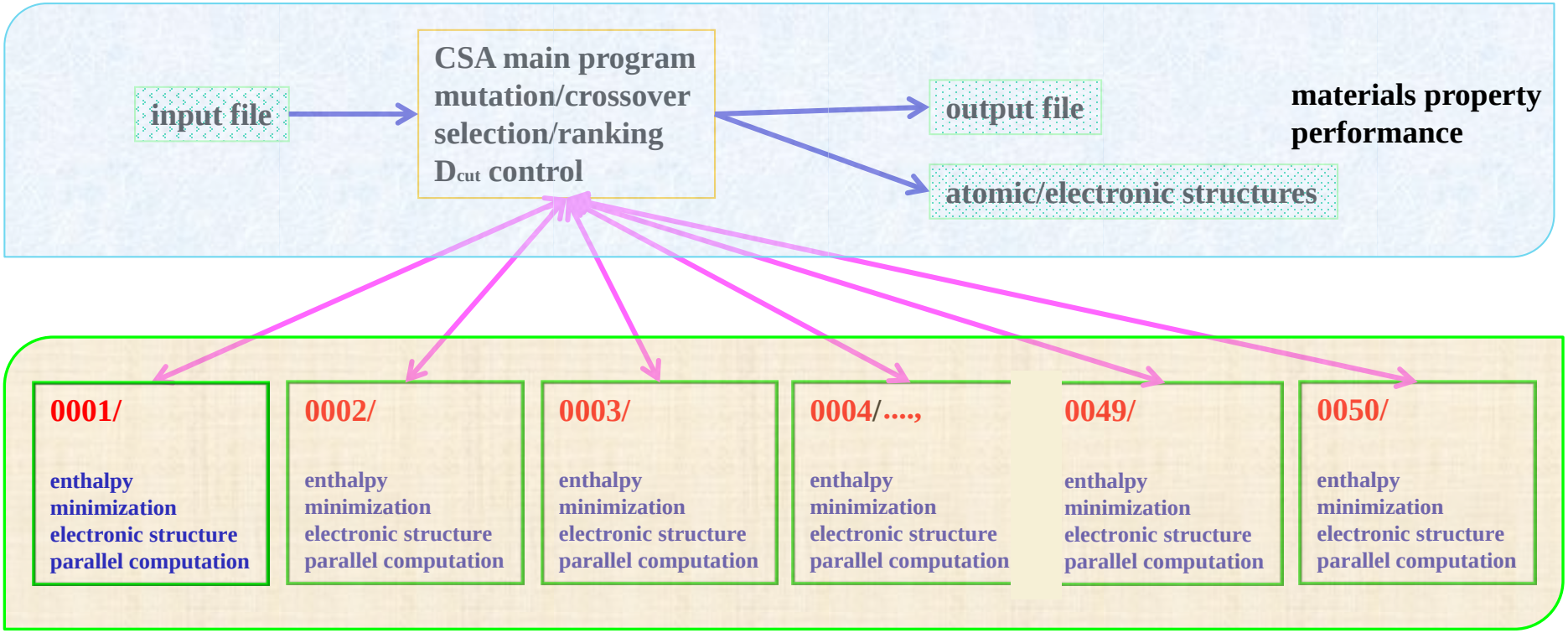

First-principles DFT calculation : many CPUs

InfiniBand
Tightly coupled CPUs

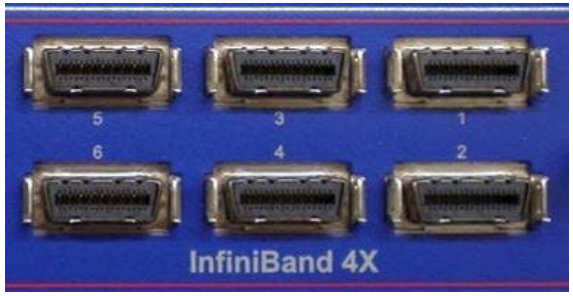

Comput. Phys. Commun. **203**, 110 (2016).


conformation 9
conformation 10
conformation 11
conformation 12
conformation 13
conformation 14
conformation 8
conformation 7
conformation 6
conformation 5
conformation 4
conformation 3
conformation 2
conformation 1

Chromosome =

$a,\ b,\ c,\ \alpha,\ \beta,\ \gamma,\ \{R_i\}$

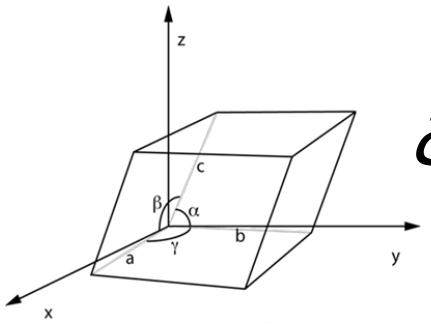

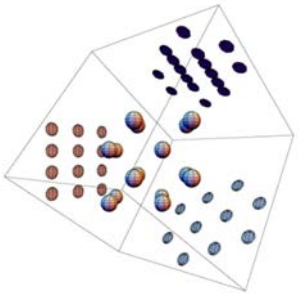

0010010110011100000

0010010110011101000

0010010110011100000

0010010110011101000

0010010110011100000

implementation

- Main driver (CSA)
- Input, restart file (iterative calculations)
- Batch (local enthalpy minimization, electronic structure)
- Parsing or syntactic analysis (output files)
- Genetic operators (crossover, mutation)
- Distance measure (bond length distribution)
- Sorting (objective function)
- Random numbers (stochastic processes)
- Many directories (“parallel in parallel”)
- Different CPU amounts for different local enthalpy minimizations

Comput. Phys. Commun. **203**, 110 (2016).

KRISS

Population size (fixed); iterative

- Crystal structures, objective functions
- Ranking (objective function)
- Diversity check (distance)
- Random symmetric structures (initial)
- 1 ~ 230 space group (random)

Comput. Phys. Commun. **203**, 110 (2016).

Chromosome = a, b, c, α, β, γ, $\{R_i\}$

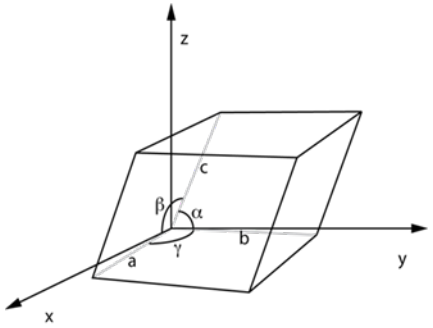

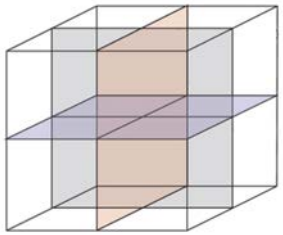

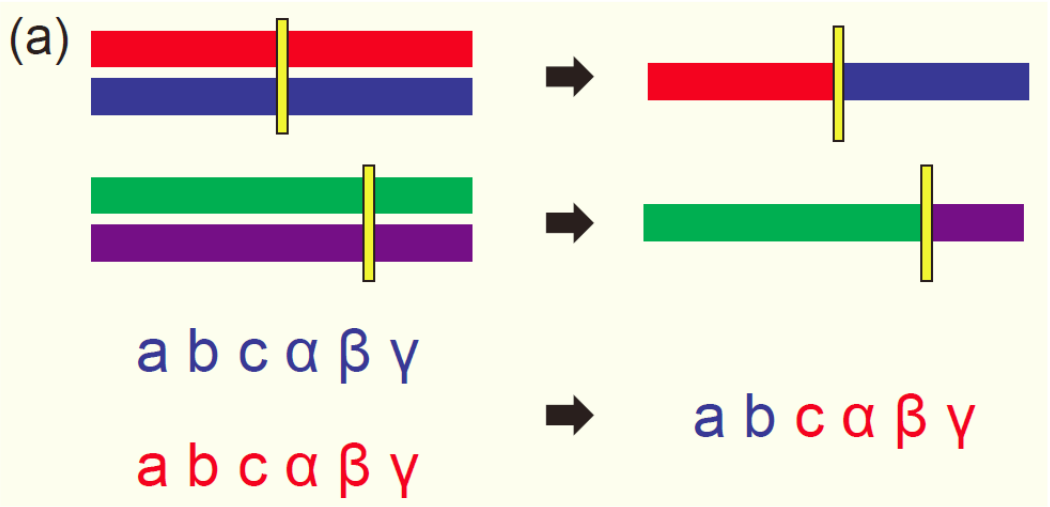

Comput. Phys. Commun. **203**, 110 (2016).

KRISS

crossover/mutation

- One-dimensional representation
- Chromosome = a, b, c, α, β, γ, $\{R_i\}$
- Crossover (1/2+1/2, 1/4 +3/4) ; random rotations (one-dimensional representation)
- Mutation (long-range, short-range, Gaussian)
- Mutation : Crossover= 2 : 8
- Core-core cure (Monte Carlo)

$$20^\circ \le \alpha \le 160^\circ,\ 20^\circ \le \beta \le 160^\circ,\ 20^\circ \le \gamma \le 160^\circ,$$

$$a > 1.2\ \text{Å},\ b > 1.2\ \text{Å},\ c > 1.2\ \text{Å},$$

$$0.3 \le a/b \le 6.0,\ 0.3 \le b/c \le 6.0,\ 0.3 \le c/a \le 6.0.$$

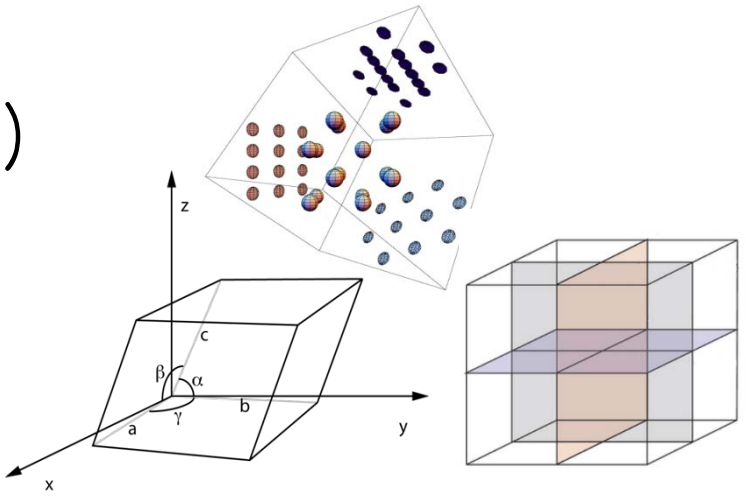

Comput. Phys. Commun. **203**, 110 (2016).

KRISS

Diversity and distance

- New type and/or low objective function
- Distance cutoff value (annealing)
- Replacement (old-type), introduction (new-type)
- Hamming distance

Comput. Phys. Commun. **203**, 110 (2016).

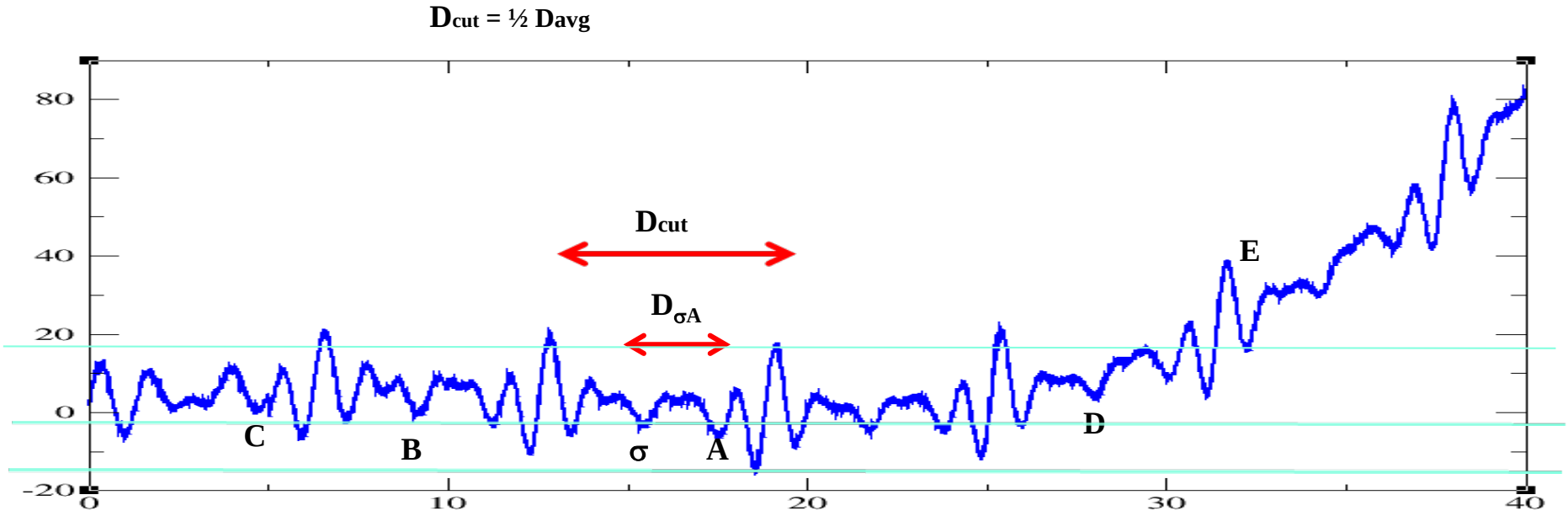

Trial conformation: σ
Bank conformations: A, B, C, D, and E

The closest conformation *A* (to σ) at a distance $D_{\sigma A}$.
- **If $D_{\sigma A} < D_{cut}$, σ replaces *A* if σ is lower in energy than *A*.**
- **If $D_{\sigma A} > D_{cut}$, σ replaces *E*, the highest energy conformation in the bank, if σ, in addition, is lower in energy than *E*.**
- **If σ does not satisfy the "lower in energy" condition in either of the two cases, σ is discarded.**

$D_{cut} \leftarrow D_{cut} \times 0.99$

Comput. Phys. Commun. **203**, 110 (2016).

Programming details

- string treatment
- directory generation
- PBS job submission
- system call
- file: inquire, delete
- sleep
- batch
- fault-tolerant mode

Programming details

- http://incredible.egloos.com/4836430
- http://incredible.egloos.com/5008405
- http://incredible.egloos.com/3044815
- http://incredible.egloos.com/4790690
- http://incredible.egloos.com/6208916
- http://incredible.egloos.com/4837144
- http://incredible.egloos.com/5074249

Solar cell

- In one day, the irradiation from the sun on the earth gives about 10,000 times more energy than the daily use from mankind.
- A **solar cell** (also called a **photovoltaic cell** or **photocell**) is an electrical device that converts the energy of light directly into electricity by the photovoltaic effect.
- Semiconductors with bandgap between 1 and 1.5 eV, or near–infrared light, have the greatest potential to form an efficient cell.

Near infrared : 0.75–1.4 μm , 0.9–1.7 eV
Far infrared : 15–1,000 μm, 1.2–80 meV

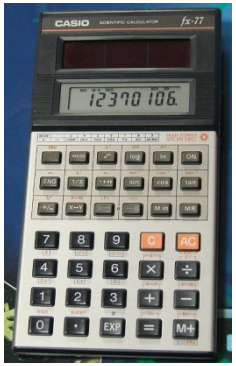

Light comparison			
Name	**Wavelength**	**Frequency (Hz)**	**Photon Energy (eV)**
Gamma ray	less than 0.01 nm	more than 30 EHz	124 keV – 300+ GeV
X-Ray	0.01 nm – 10 nm	30 EHz – 30 PHz	124 eV – 124 keV
Ultraviolet	10 nm – 380 nm	30 PHz – 790 THz	3.3 eV – 124 eV
Visible	380 nm–700 nm	790 THz – 430 THz	1.7 eV – 3.3 eV
Infrared	700 nm – 1 mm	430 THz – 300 GHz	1.24 meV – 1.7 eV
Microwave	1 mm – 1 meter	300 GHz – 300 MHz	1.24 μeV – 1.24 meV
Radio	1 mm – 100,000 km	300 GHz – 3 Hz	12.4 feV – 1.24 meV

Solar Energy Materials & Solar Cells **100**, 69 (2012).

http://en.wikipedia.org/wiki/Infrared
http://en.wikipedia.org/wiki/Solar_cell

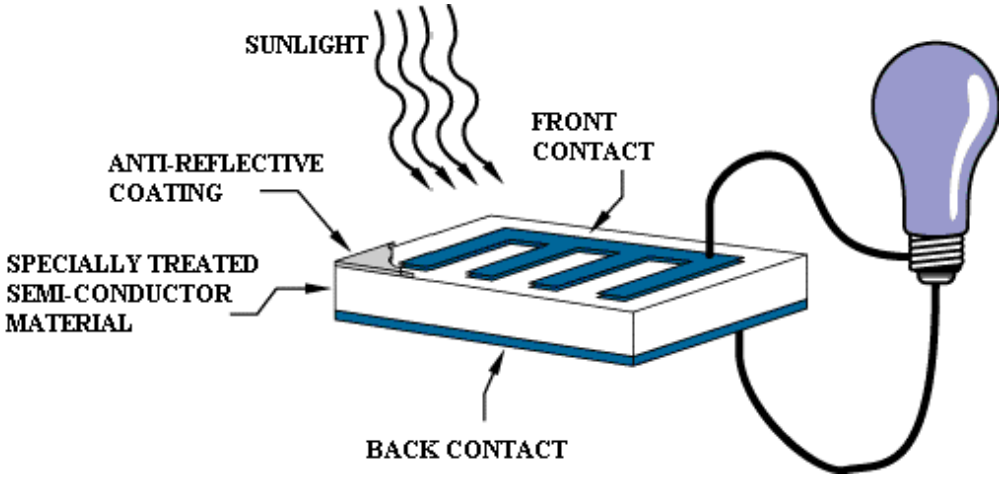

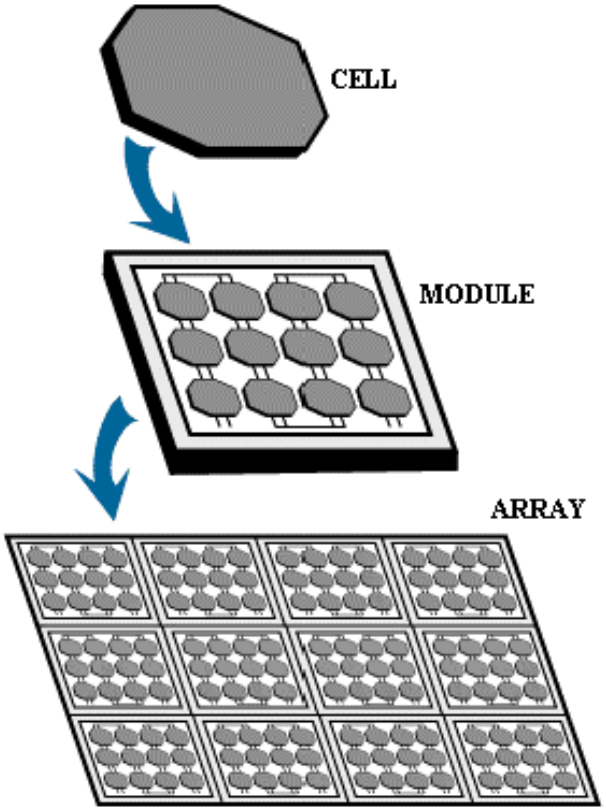

c-Si, thickness : 160–240 μm

To make an efficient solar cell, we try to maximize absorption, minimize reflection and recombination, and thereby maximize conduction.

http://science1.nasa.gov/science-news/science-at-nasa/2002/solarcells/

photovoltaic energy production

- Direct band gap 1.0~1.5 eV (absorption properties for solar light)

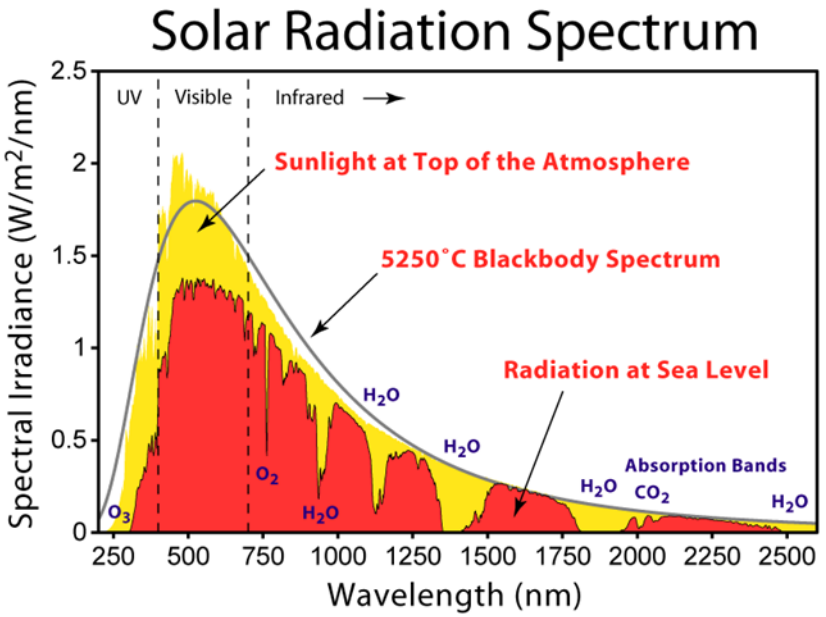

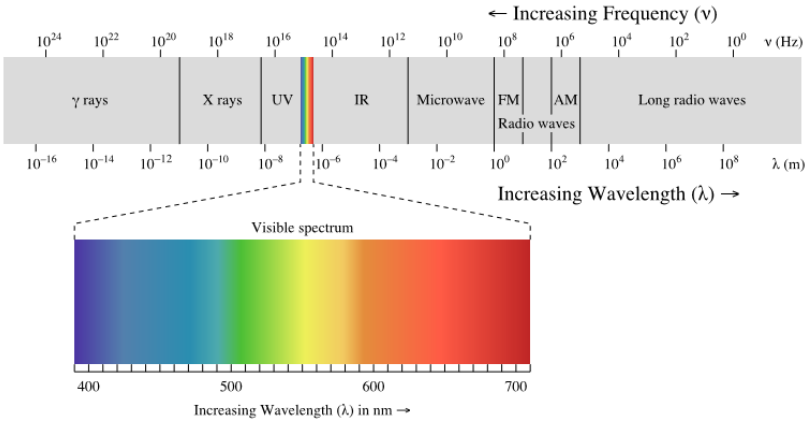

http://en.wikipedia.org/wiki/Sun_light
http://en.wikipedia.org/wiki/Light

Shockley–Queisser limit

(detailed balance limit)

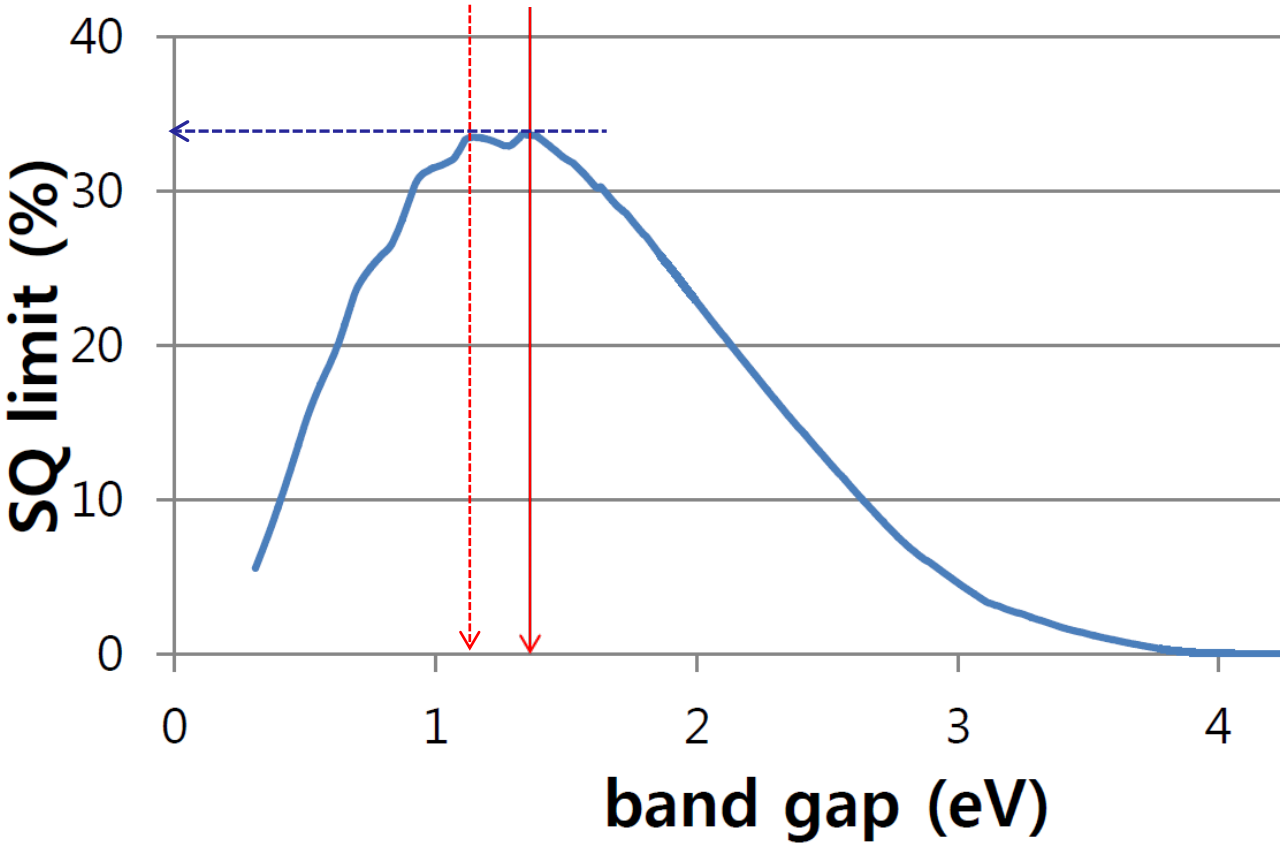

Of all the power contained in sunlight falling on an ideal solar cell (about 1000 W/m^2), only 33.7% of that could ever be turned into electricity (337 W/m^2).

J. Appl. Phys. **32**, 510 (1961). **http://en.wikipedia.org/wiki/Shockley%E2%80%93Queisser_limit**

KRISS

Objective function

Objective function = $-E_g^i + \mathrm{Max}[0, (E_g^d - E_g^i)]$

Indirect band gap size

Direct band gap size

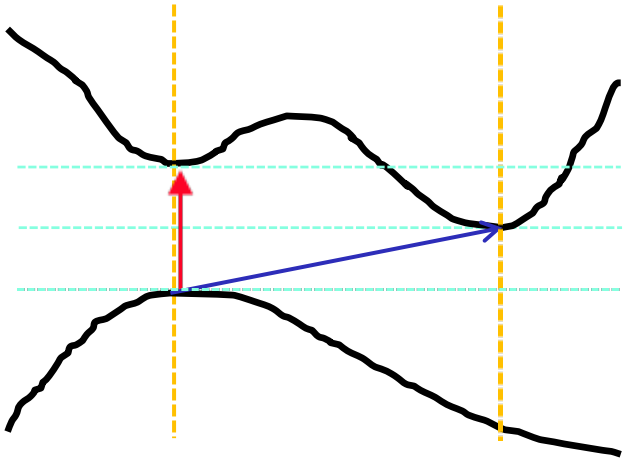

Objective function = $-E_g^i + \mathrm{Max}[0, (E_g^d - E_g^i)] + P$

$$P(a, b, c, \alpha, \beta, \gamma, \{\vec{R}_I\}) = \begin{cases} 0.5 - E_g^d, & \text{if } E_g^d \leq 0.5 \\ E_g^d - 0.8. & \text{if } E_g^d \geq 0.8 \end{cases}$$

Phys. Rev. B **90**, 115209 (2014); Comput. Phys. Commun. **203**, 110 (2016).

KRISS

Objective function

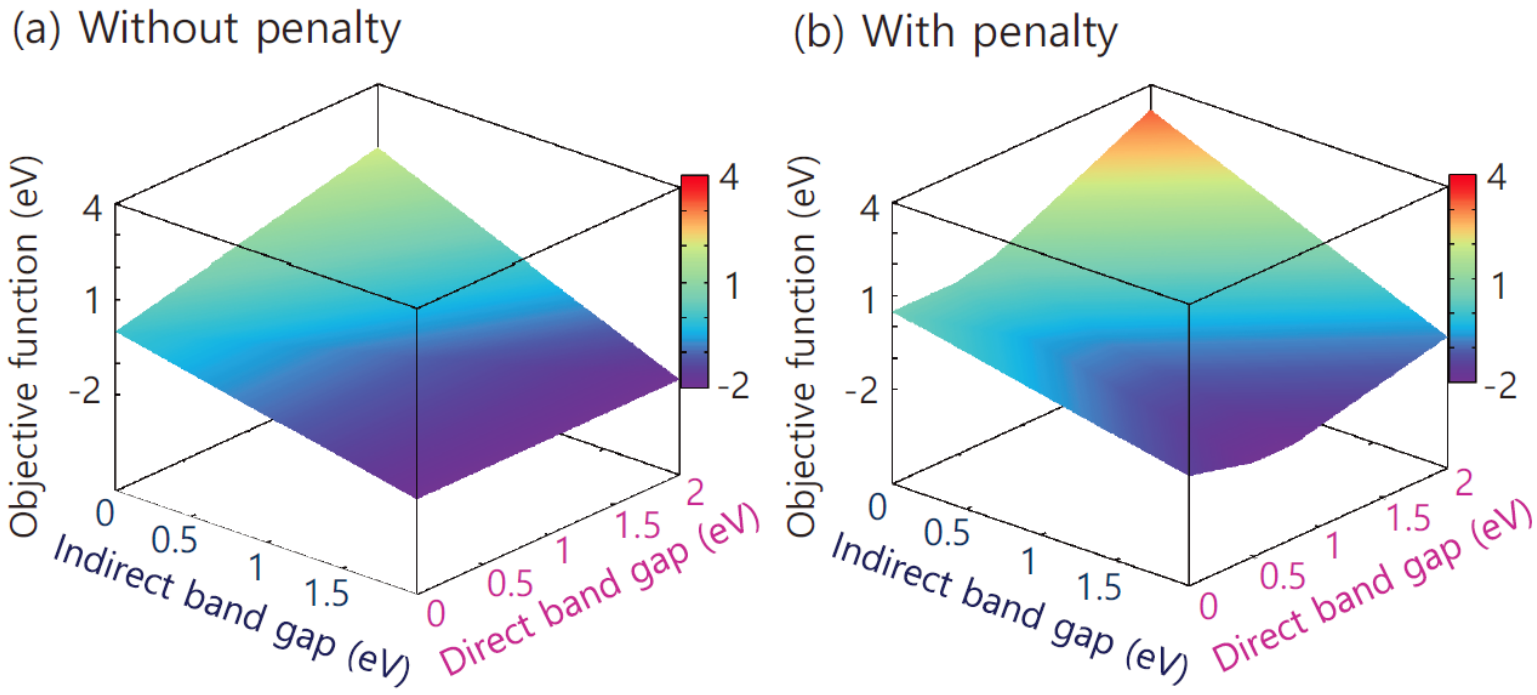

Comput. Phys. Commun. **203**, 110 (2016).

KRISS

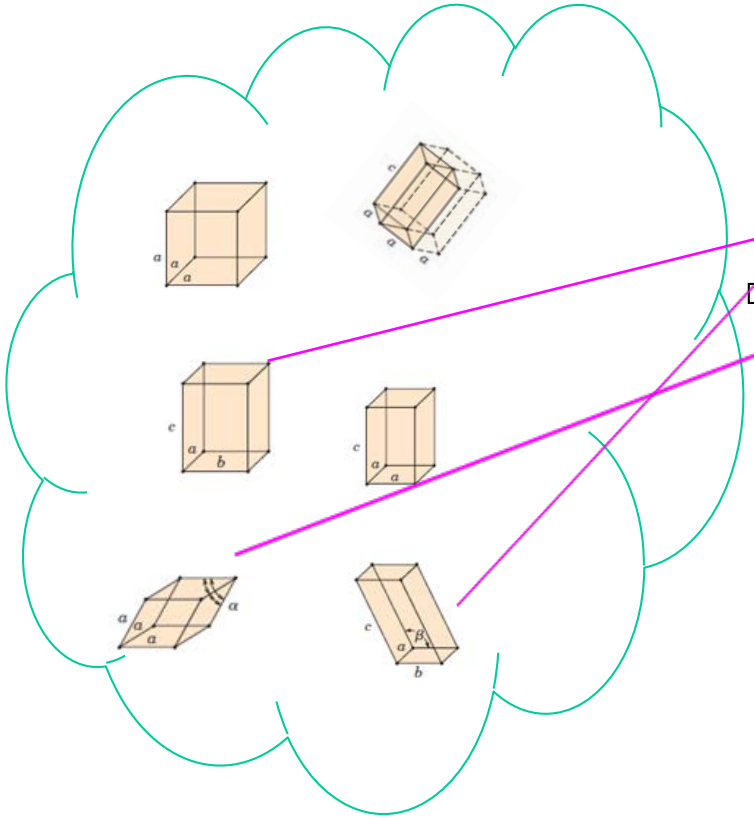

$D_{cut} = 0.5 D_{avg}$

Crossover,
Mutation,
Crossover,
Crossover,
Crossover,
Mutation,
Crossover,
…..

Enthalpy minimization,
Enthalpy minimization,
Enthalpy minimization,
Enthalpy minimization,
Enthalpy minimization,
Enthalpy minimization,
Enthalpy minimization,
Enthalpy minimization,
Enthalpy minimization,
Enthalpy minimization,
Enthalpy minimization,
Enthalpy minimization,
Enthalpy minimization,
Enthalpy minimization,
Enthalpy minimization,
Enthalpy minimization,
……

Replacement
Annealing

Comput. Phys. Commun. **203**, 110 (2016).

KRISS

Solar cell materials

- Silicon
- Direct band gap (~ 1.1 eV, 1.3 eV)
- Dipole-allowed transition
- Small lattice mismatch (< 1.0%)
- Thermal stability
- High efficiency

Abundance, crust

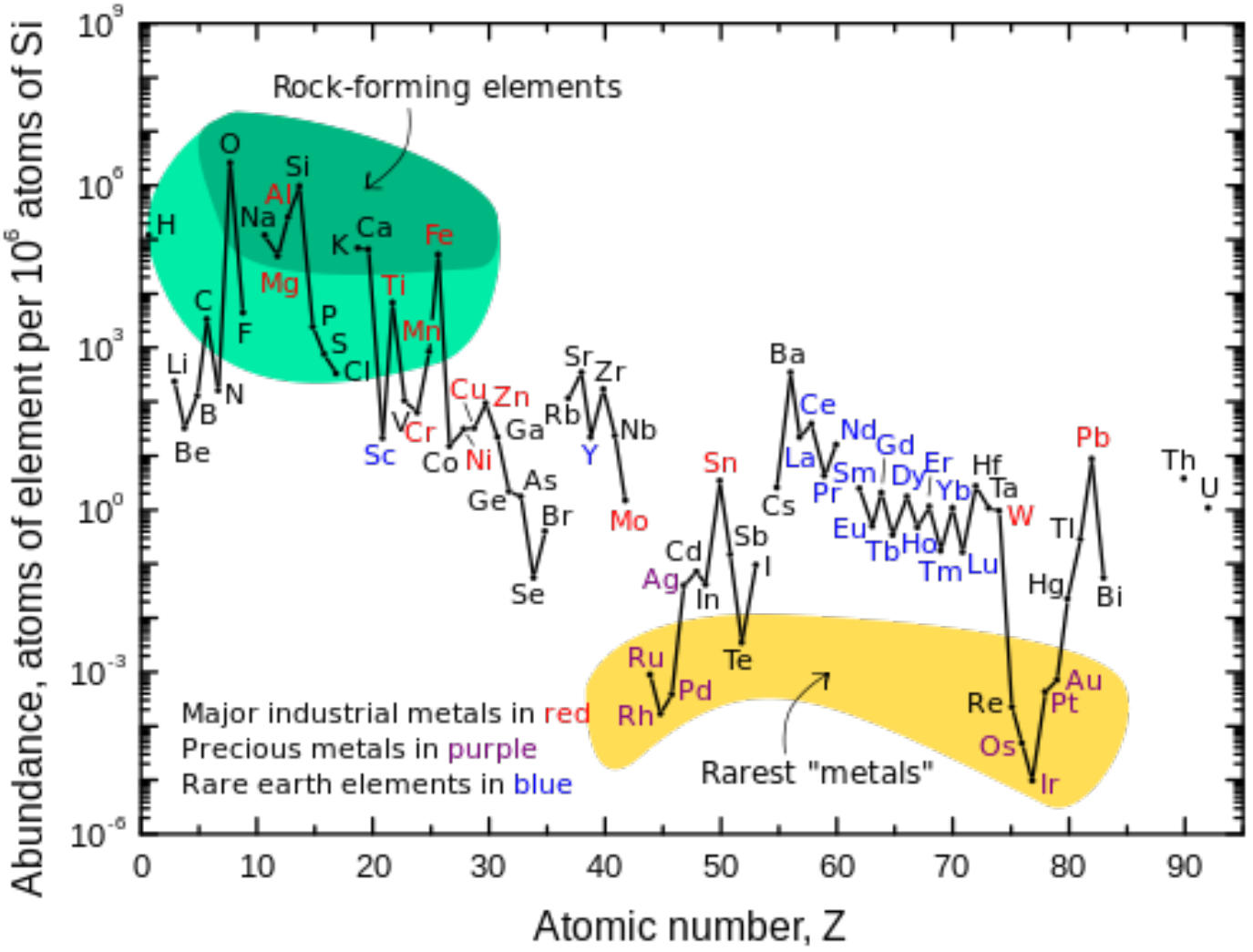

http://en.wikipedia.org/wiki/Crust_(geology)

KRISS

PN-junction type solar cell

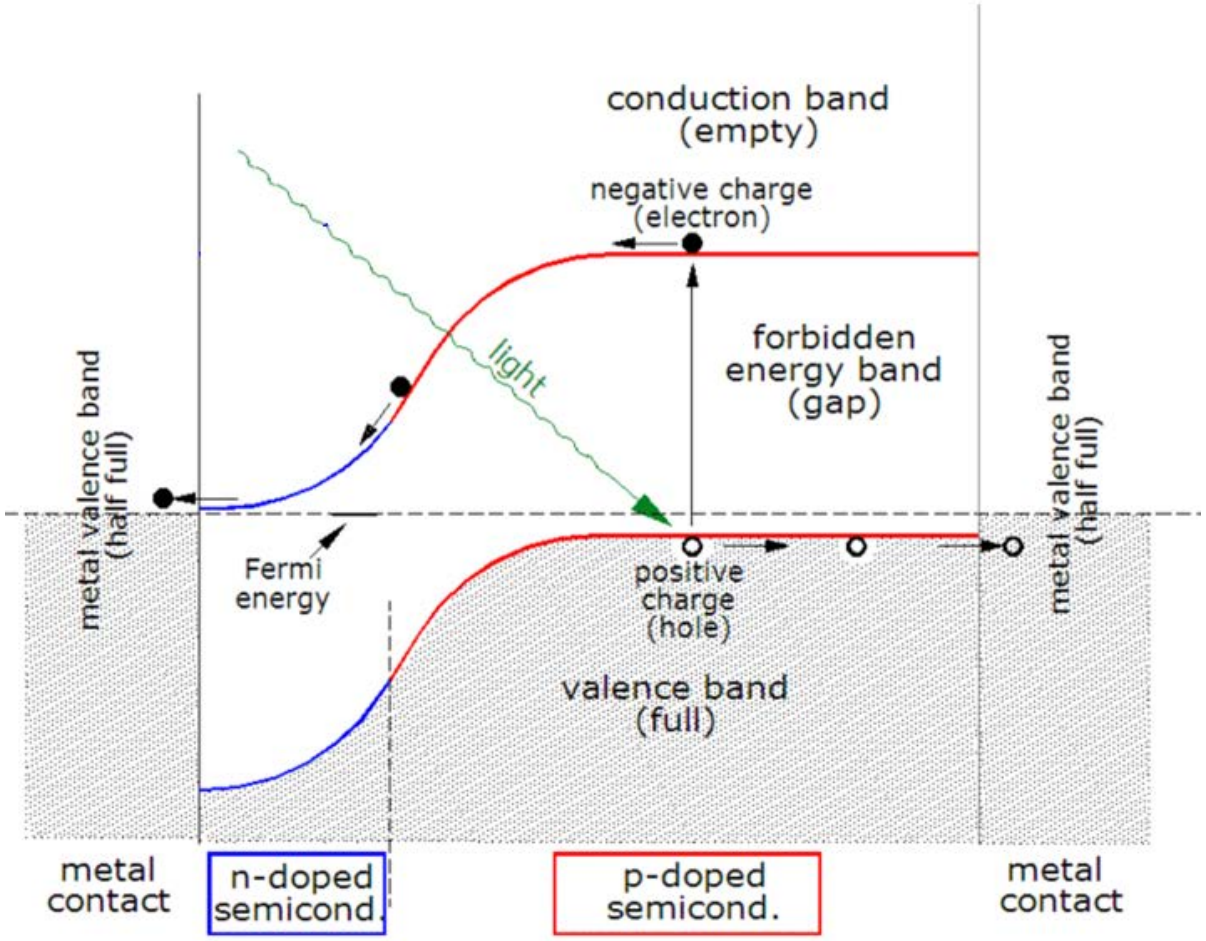

In *a*-Si, the diffusion length of minority carriers is usually very short due to the existence of defects, and the dominant charge separation is therefore drift, driven by the electrostatic field of the junction, which extends to the whole thickness of the cell.[1]

http://en.wikipedia.org/wiki/File:BandDiagramSolarCell-en.gif **(modified)**

KRISS

Absorption coefficient

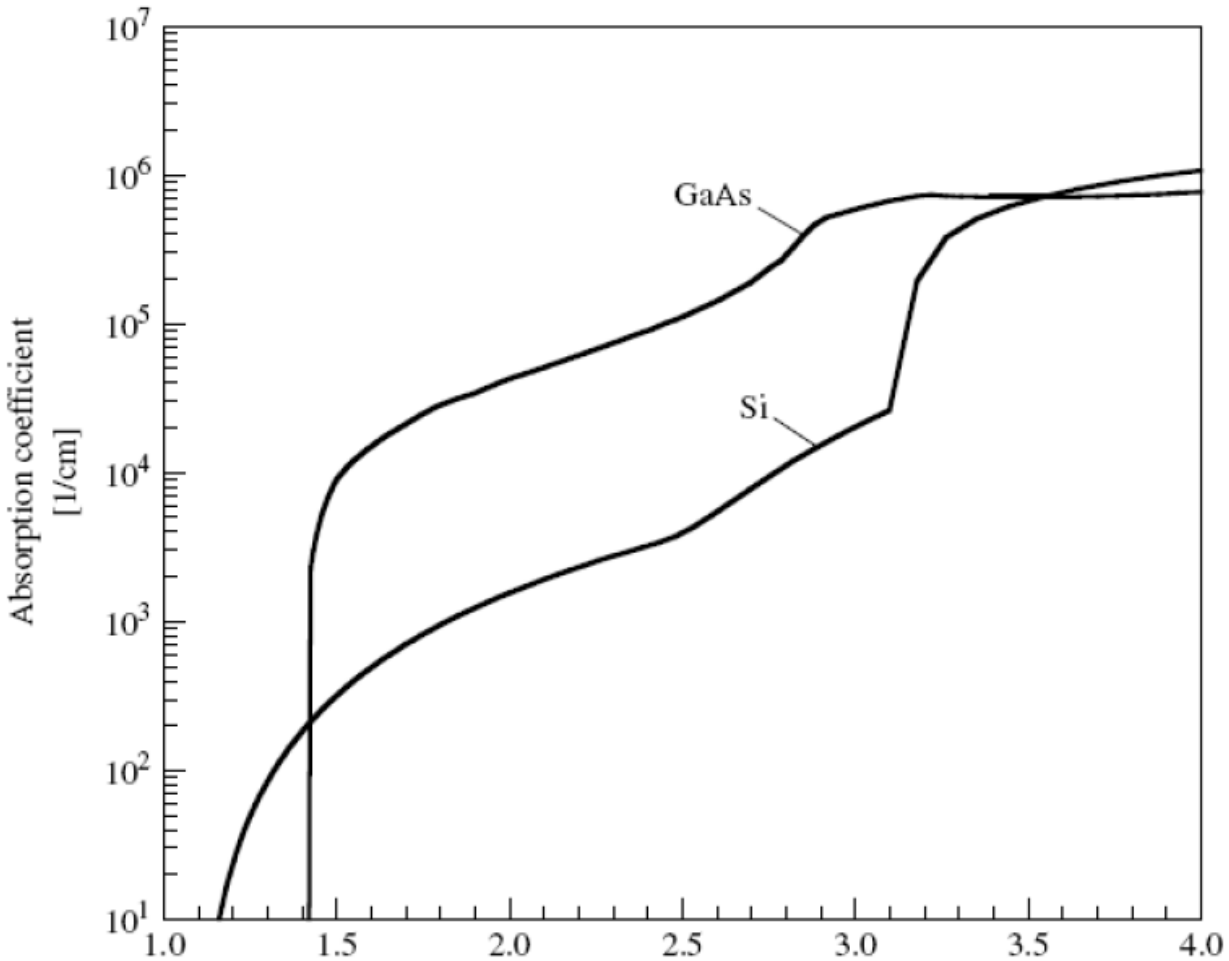

Red 620–750 nm, 400–484 THz, 1.60–2.00 eV

Violet 380–450 nm, 668–789 THz, 2.75–3.26 eV

A typical human eye will respond to wavelengths from about 390 to 700 nm.

KRISS

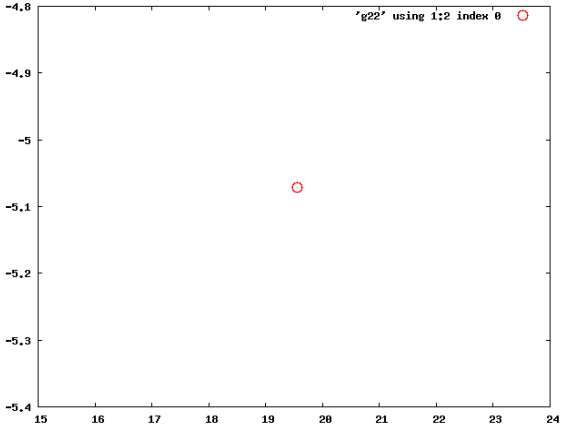

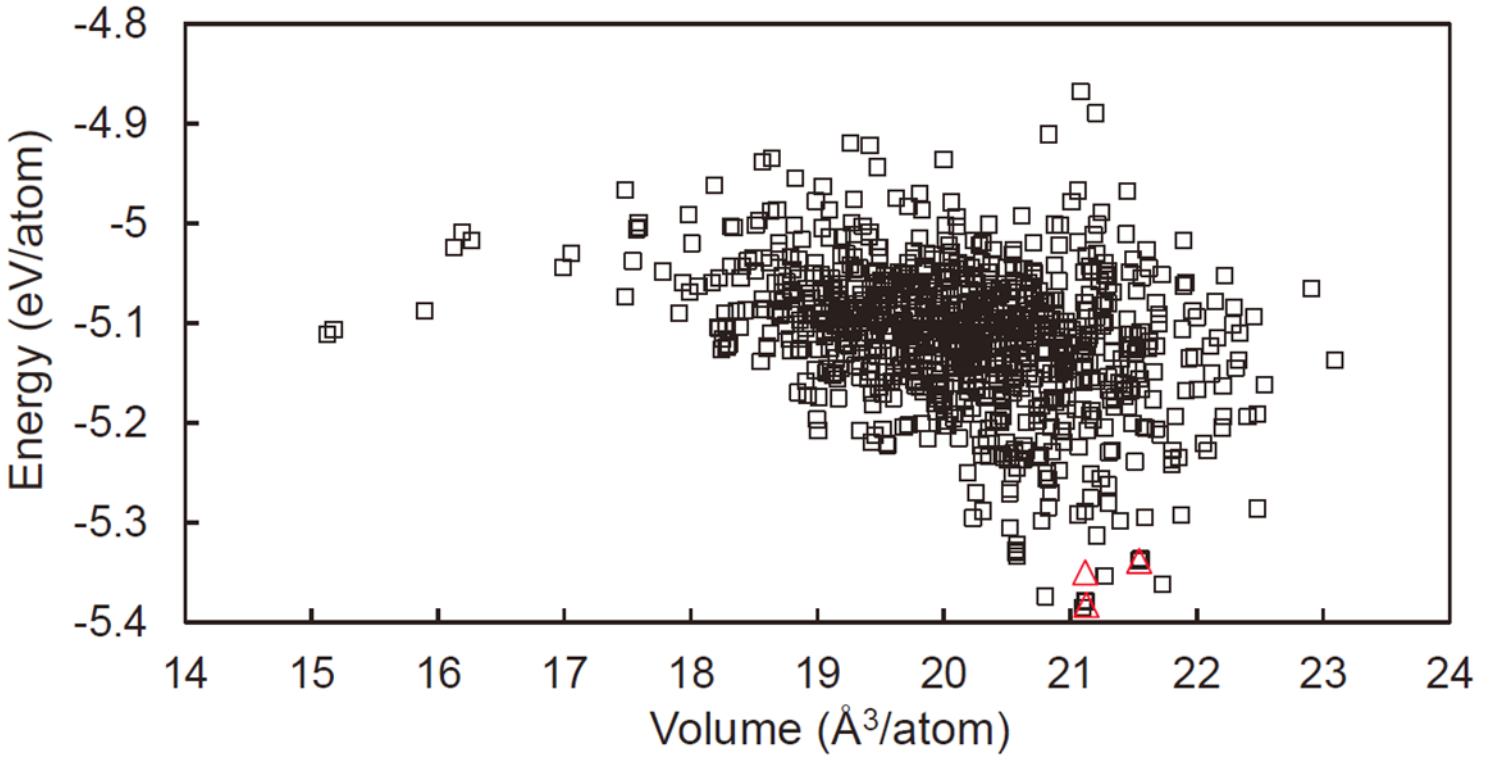

Comput. Phys. Commun. **203**, 110 (2016).

KRISS

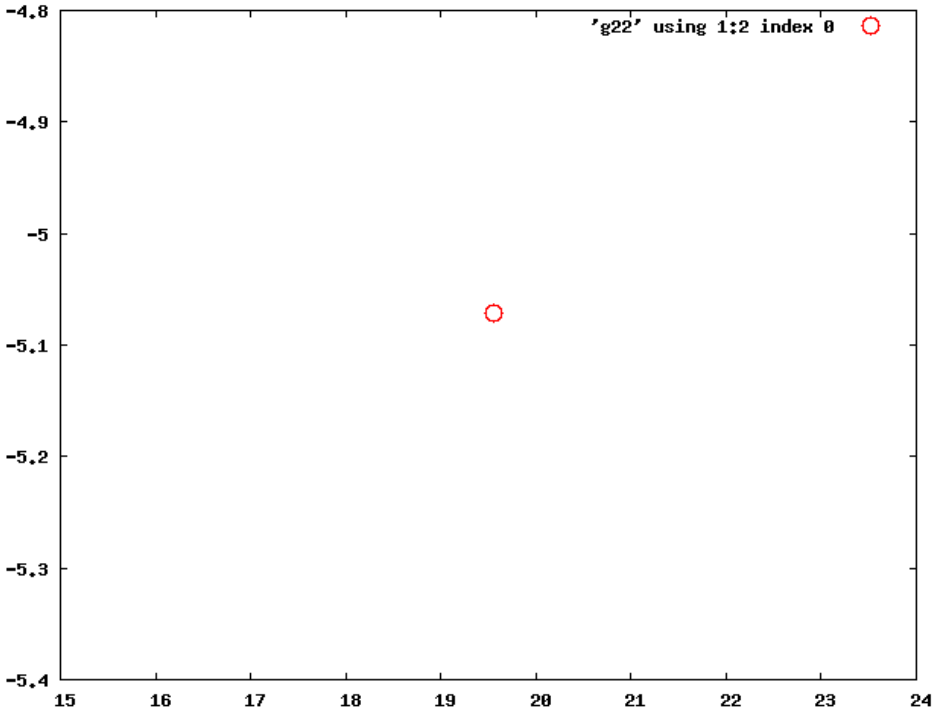

Comput. Phys. Commun. **203**, 110 (2016).

Structure	Lattice	Atoms	(Å^3/atom)	(eV/atom)	$\overline{r}$ (Å), σ_r (Å)	$\overline{\theta}$ (°), σ_θ (°)	E_g^d (eV)	E_g^i (eV)	Space group	Ref.
D262	pm	10	21.02	0.08	2.37, 0.04	109.26, 8.17	**0.29**		$P2_1/m$ (*No.* 11)	
D12	or (C)	10	21.56	0.13	2.37, 0.01	108.98, 11.19	**0.50**		$Cmmm$ (*No.* 65)	
D239	tc	10	22.72	0.16	2.37, 0.03	108.69, 13.50	**0.77**		$P1$ (*No.* 1)	
D63	bcm	12	21.10	0.12	2.37, 0.04	109.09, 9.76	**0.66**		$C2/m$ (*No.* 12)	
D135	bcm	12	21.24	0.22	2.38, 0.05	108.42, 14.73	**0.64**		Cc (*No.* 9)	
D243	tc	12	21.88	0.29	2.38, 0.04	107.29, 18.42	**0.61**		$P1$ (*No.* 1)	
D76	bcm	20	21.70	0.13	2.37, 0.03	109.01, 10.59	**0.57**		$C2$ (*No.* 5)	
D979	tc	20	21.17	0.29	2.38, 0.05	108.56, 18.40	**0.60**		$P1$ (*No.* 1)	
Q130	bcm	12	21.86	0.08	2.37, 0.02	108.97, 9.78	0.64	**0.63**	$C2/m$ (*No.* 12)	
Q135	bcm	12	21.50	0.15	2.37, 0.04	108.95, 11.78	**0.93**		$C2/c$ (*No.* 15)	
Q465	tc	12	21.85	0.13	2.37, 0.02	109.06, 13.63	1.25	**1.23**	$P\bar{1}$ (*No.* 2)	
Q1102	pm	12	21.55	0.14	2.37, 0.02	109.19, 13.97	1.33	**1.20**	Pc (*No.* 7)	
Q419	tc	12	22.25	0.20	2.38, 0.03	108.71, 14.11	1.26	**1.11**	$P1$ (*No.* 1)	
Q8	tc	14	20.35	0.30	2.39, 0.05	108.84, 17.19	0.65	**0.56**	$P1$ (*No.* 1)	
Q57	tc	14	21.55	0.34	2.39, 0.05	107.77, 18.95	0.34	**0.23**	$P1$ (*No.* 1)	
Q1377	tc	16	21.15	0.28	2.39, 0.05	108.23, 14.43	0.34	**0.26**	$P1$ (*No.* 1)	
Q913	tc	18	20.83	0.26	2.38, 0.05	108.56, 16.63	0.91	**0.77**	$P1$ (*No.* 1)	
Q833	tc	18	20.94	0.26	2.38, 0.03	108.07, 15.59	0.73	**0.69**	$P1$ (*No.* 1)	
Q1023	tc	18	20.37	0.28	2.40, 0.06	106.15, 17.60	0.30	**0.17**	$P1$ (*No.* 1)	
Q50	tc	18	20.54	0.31	2.39, 0.06	108.82, 17.99	0.51	**0.41**	$P1$ (*No.* 1)	
Q78	or	20	21.64	0.11	2.37, 0.01	109.26, 11.42	0.74	**0.69**	$Pma2$ (*No.* 28)	
Q636	tc	20	20.89	0.15	2.38, 0.04	109.09, 10.79	0.96	**0.84**	$P1$ (*No.* 1)	
Q736	tc	20	20.89	0.16	2.37, 0.04	109.26, 11.07	0.92	**0.78**	$P1$ (*No.* 1)	
Q85	tc	20	20.11	0.21	2.38, 0.05	109.13, 13.15	0.69	**0.58**	$P1$ (*No.* 1)	
Q202	tc	20	20.13	0.22	2.38, 0.05	109.41, 12.55	0.47	**0.43**	$P1$ (*No.* 1)	
Q7	tc	20	20.43	0.22	2.38, 0.05	109.16, 13.38	0.54	**0.44**	$P1$ (*No.* 1)	
Q108	tc	20	21.19	0.23	2.38, 0.05	108.74, 13.74	0.69	**0.67**	$P1$ (*No.* 1)	
Q660	tc	20	20.95	0.30	2.39, 0.06	106.53, 18.76	0.34	**0.31**	$P1$ (*No.* 1)	
I391	pm	12	22.29	0.12	2.37, 0.02	109.15, 11.31	1.09	**0.91**	$P21/m$ (*No.* 11)	
I512	pm	12	22.61	0.16	2.37, 0.02	108.65, 12.58	1.12	**0.95**	Pm (*No.* 6)	
I241	pm	12	18.33	0.18	2.39, 0.01	108.48, 16.45	1.08	**0.85**	$P21/c$ (*No.* 14)	
I1373	bct	14	21.73	0.06	2.37, 0.02	109.19, 8.30	1.66	**1.29**	$I\bar{4}$ (*No.* 82)	
I713	tc	14	21.67	0.26	2.38, 0.05	108.62, 14.78	0.75	**0.43**	$P1$ (*No.* 1)	
I844	tc	14	20.99	0.28	2.38, 0.04	107.76, 18.10	0.86	**0.70**	$P1$ (*No.* 1)	
I926	bcm	16	21.47	0.07	2.37, 0.02	109.32, 7.80	1.31	**1.10**	$C2/m$ (*No.* 12)	
I1229	tc	16	20.61	0.11	2.37, 0.04	109.20, 9.18	0.89	**0.62**	$P\bar{1}$ (*No.* 2)	
I1233	tc	16	20.76	0.16	2.37, 0.03	108.84, 10.93	1.00	**0.69**	$P1$ (*No.* 1)	
I671	tc	18	20.68	0.14	2.38, 0.04	109.21, 10.68	1.34	**0.97**	$P1$ (*No.* 1)	
I617	tc	18	21.22	0.23	2.38, 0.04	108.99, 15.13	0.56	**0.38**	$P1$ (*No.* 1)	
I83	tc	18	20.65	0.25	2.38, 0.05	108.93, 15.16	0.79	**0.50**	$P1$ (*No.* 1)	
I16	pm	20	20.72	0.12	2.37, 0.04	109.23, 9.30	0.92	**0.68**	$P2_1$ (*No.* 4)	
I257	tc	20	20.58	0.16	2.38, 0.04	109.20, 10.96	0.80	**0.63**	$P1$ (*No.* 1)	
Si_{20}-T	sc	20	21.35	0.29	2.36, 0.01	109.03, 19.02	0.99	**0.97**	$P2_13$ (*No.* 198)	[9]
$NaSi_6$ w/o Na	or	12	21.97	0.09	2.37, 0.01	109.00, 10.08	**0.58**	0.50	$Cmcm$ (*No.* 63)	[22]
Si-III (BC8)	bcc	8	18.44	0.16	2.38, 0.02	108.23, 9.52		−0.12	$Ia\bar{3}$ (*No.* 206)	[23]
Si-XII (R8)	rho	8	18.20	0.16	2.38, 0.02	107.67, 13.02		−0.28	$R\bar{3}$ (*No.* 148)	[24]
clathrate-I	sc	46	23.24	0.06	2.37, 0.01	109.34, 5.07	1.312	**1.307**	$Pm\bar{3}n$ (*No.* 223)	[25]
a-Si				0.28	2.38, 0.08	108.32, 15.5				[26]
a-Si				0.25	2.35, 0.09	108.64, 14.04				[27]
a-Si						108.6, 11.3				[28]
diamond Si										
calc.	fcc	2	20.46	0.00	2.37, 0.00	109.47, 0.00	2.56	**0.62**	$Fd\bar{3}m$ (*No.*227)	
expt.			20.01				3.40	**1.17**		[29]

Phys. Rev. B **90**, 115209 (2014).

KRISS

Examples of Si crystals with direct band gaps

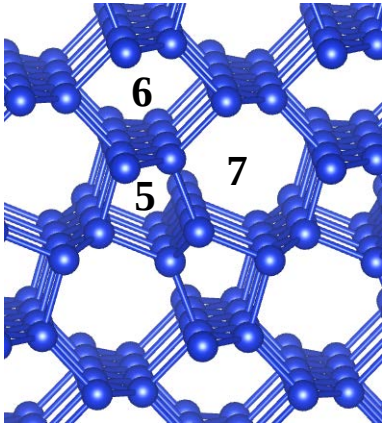

D262

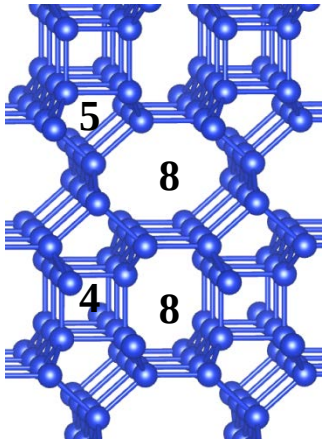

D12

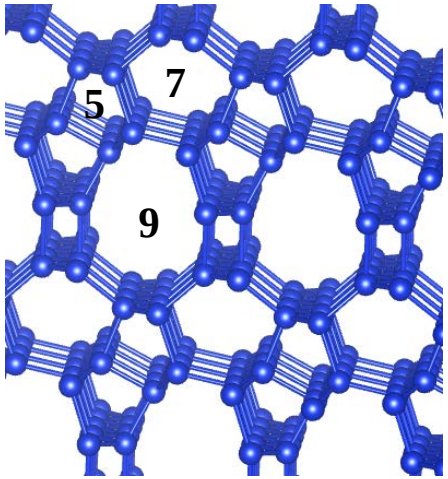

D239

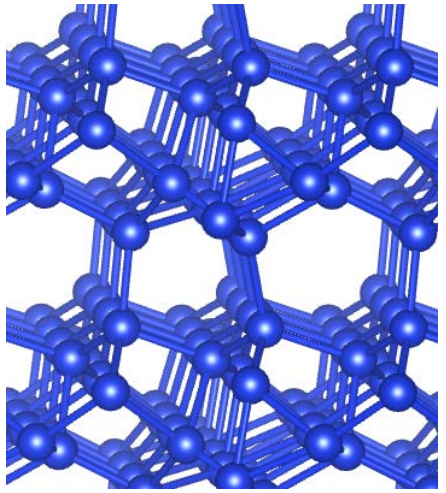

D243

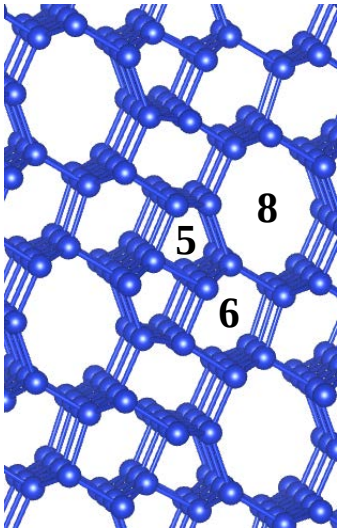

D63

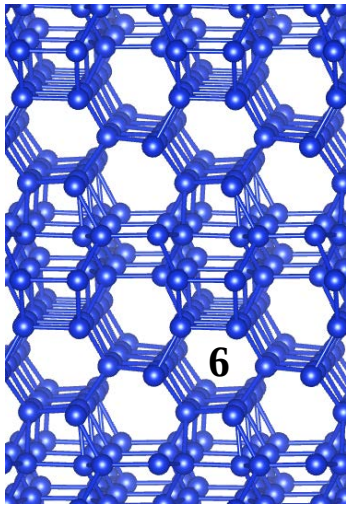

D76

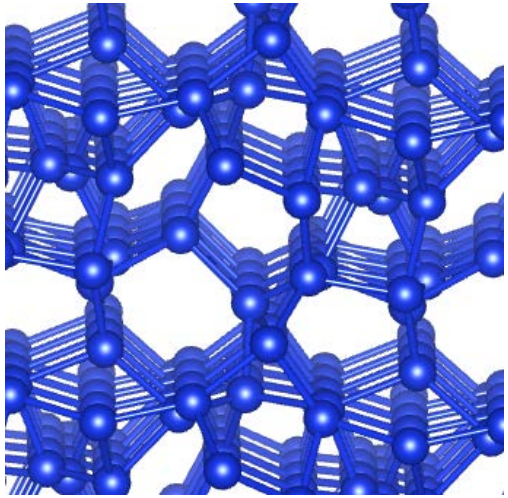

D979

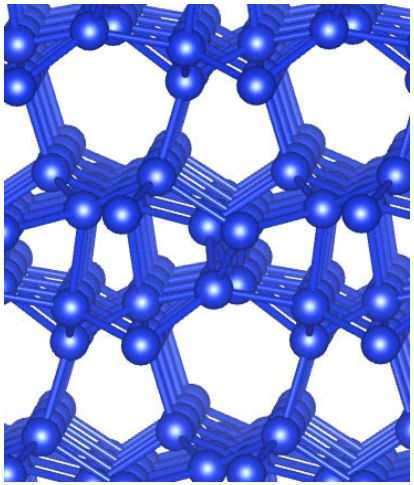

D135

- **8 crystals with direct band gaps**
- **20 crystals with quasi-direct band gaps**
- **No coordination defect in all the designed structures**

Comput. Phys. Commun. **203**, 110 (2016).

KRISS

Examples of Si crystals with direct band gaps

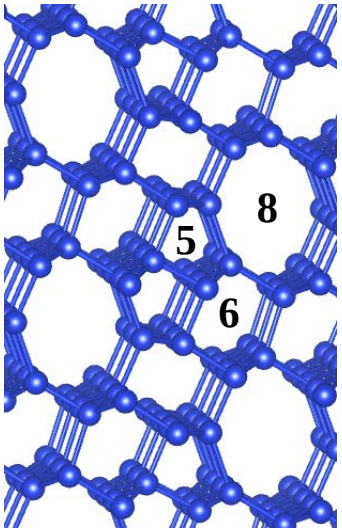

D63

(a) D63

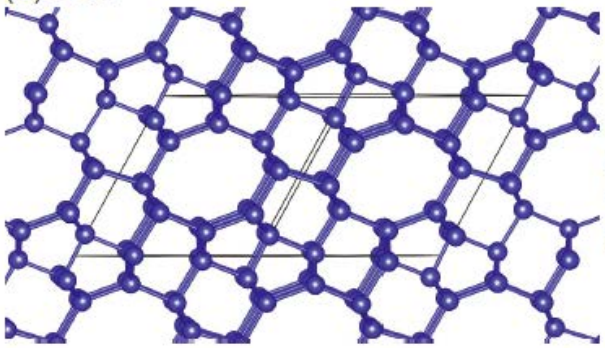

a = 17.35 Å,
b = 3.86 Å,
c = 8.64 Å,
β = 118.96°

(b) D63 with additional atoms in 8-memebered rings

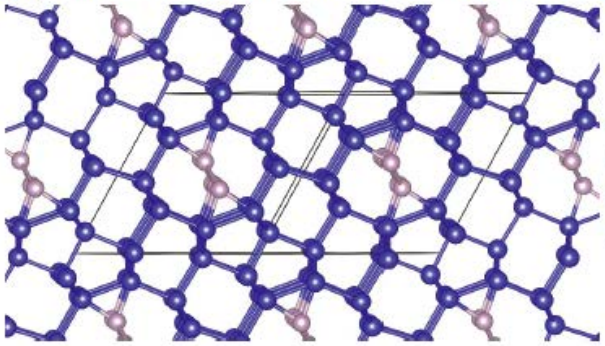

a = 17.35 Å,
b = 3.86 Å,
c = 8.64 Å,
β = 118.96°

(c) cubic diamond

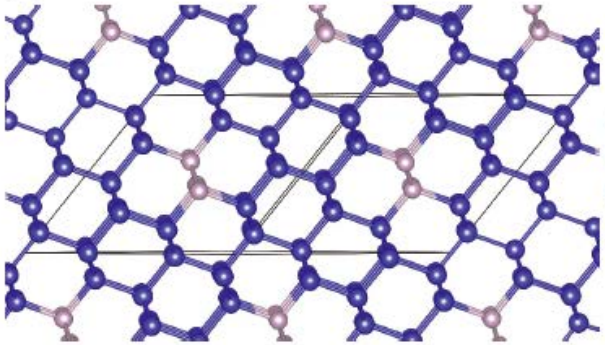

a = 16.84 Å,
b = 3.86 Å,
c = 9.47 Å,
β = 112.0°

Comput. Phys. Commun. **203**, 110 (2016).

KRISS

Direct, quasi-direct, and indirect

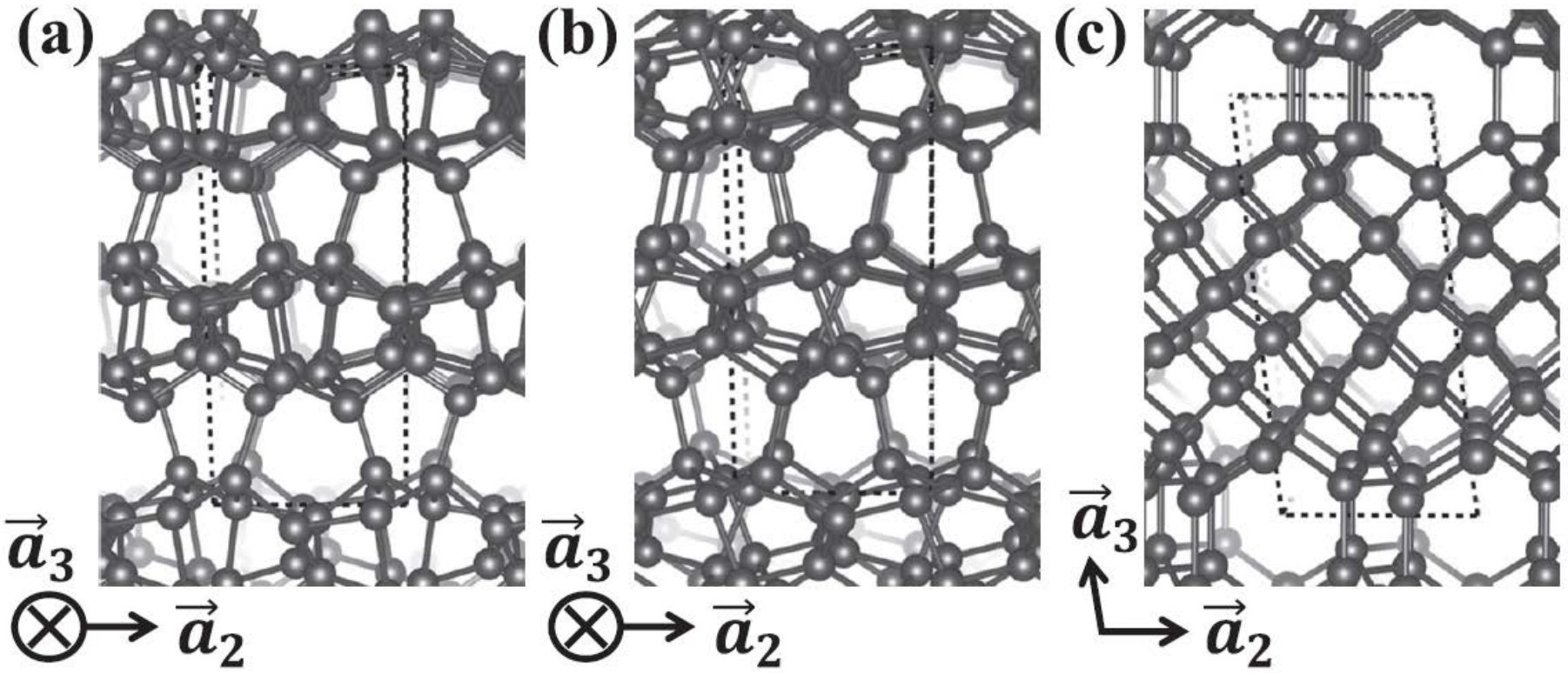

Phys. Rev. B **90**, 115209 (2014).

KRISS

Direct, quasi-direct, and indirect

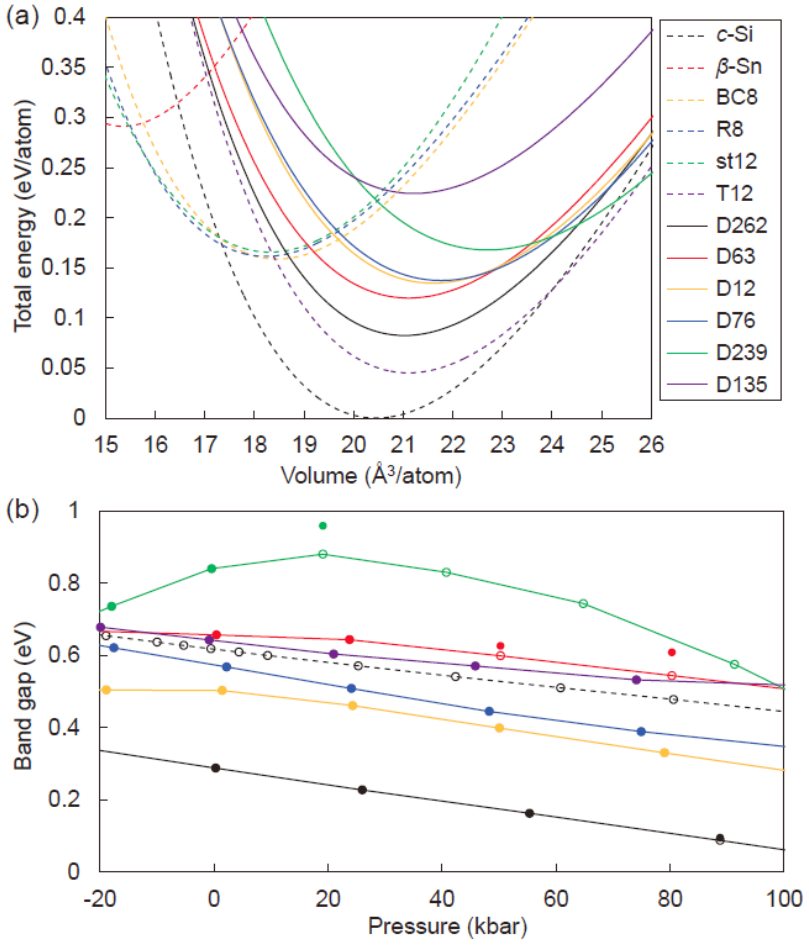

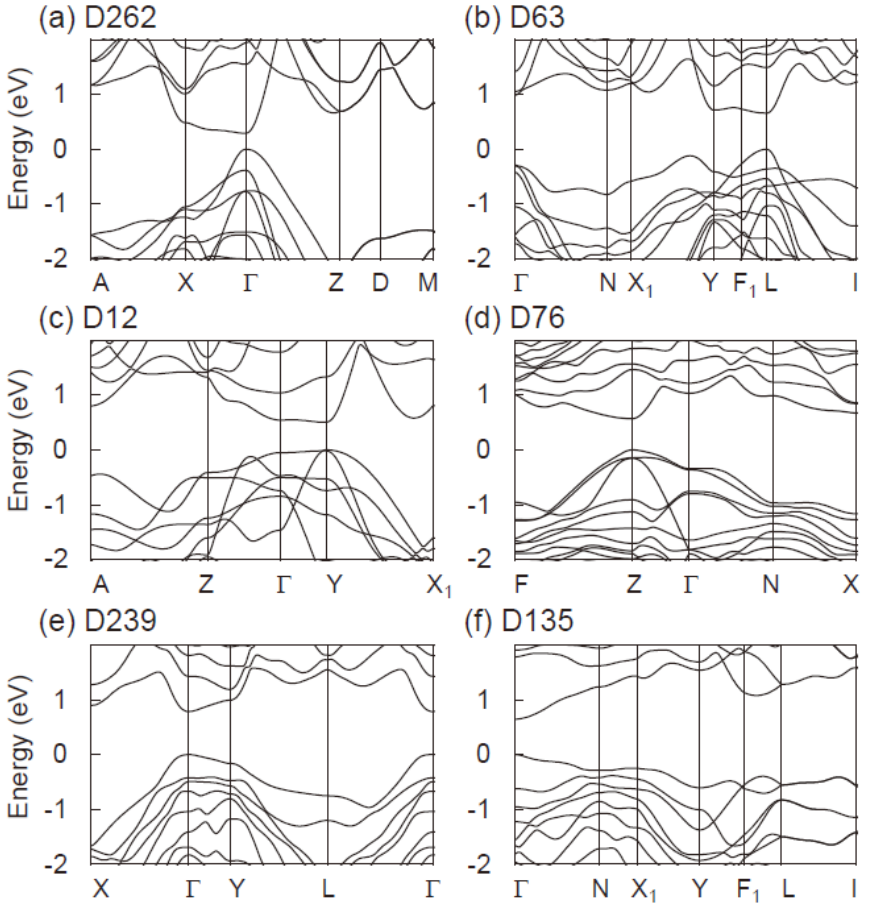

Phys. Rev. B **90**, 115209 (2014); Comput. Phys. Commun. **203**, 110 (2016).

Energy vs volume, bandgap vs pressure

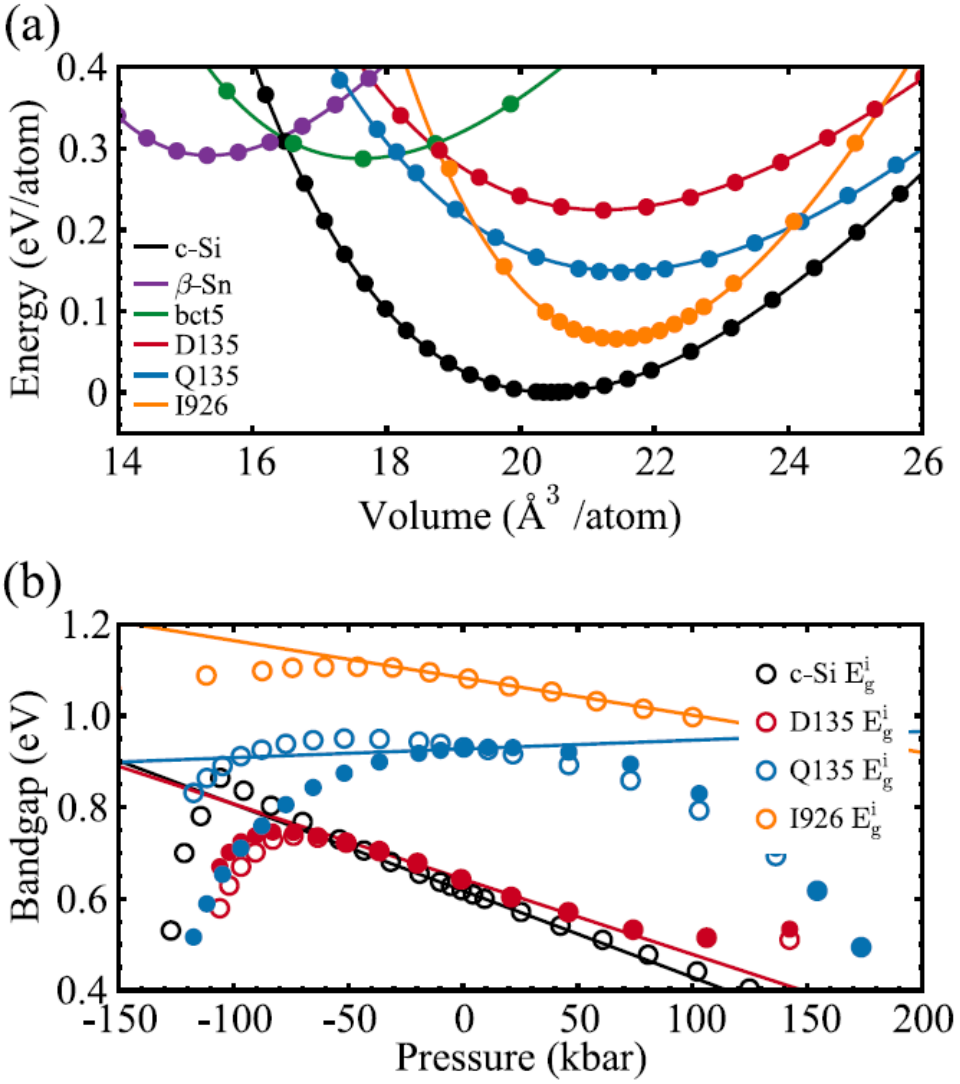

Phys. Rev. B **90**, 115209 (2014).

KRISS

Dynamical stability, band structure

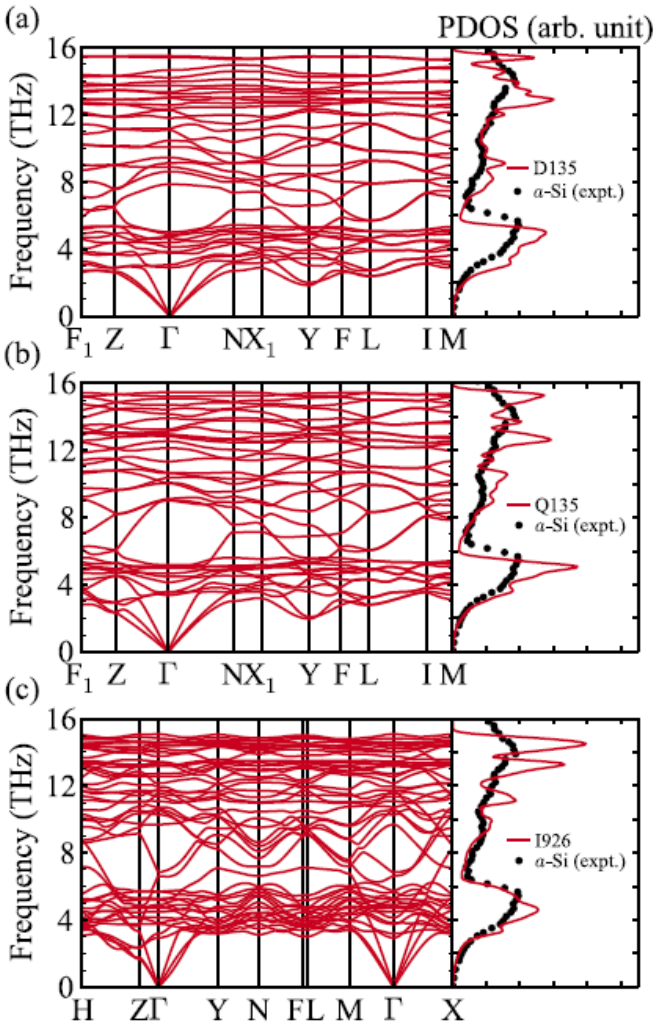

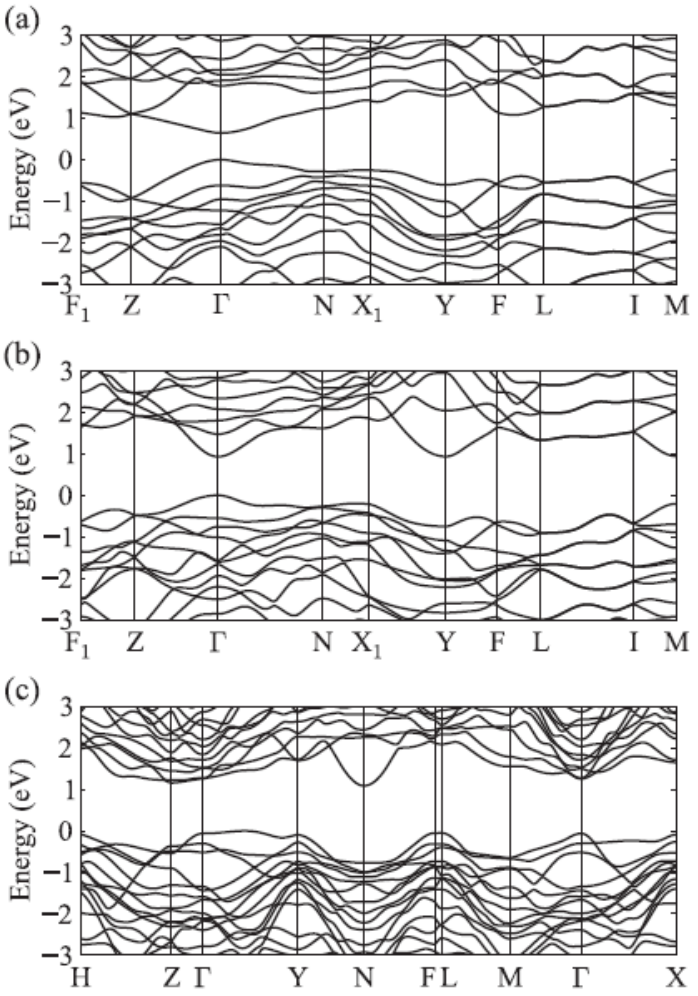

Phys. Rev. B **90**, 115209 (2014).

KRISS

Thermal stability

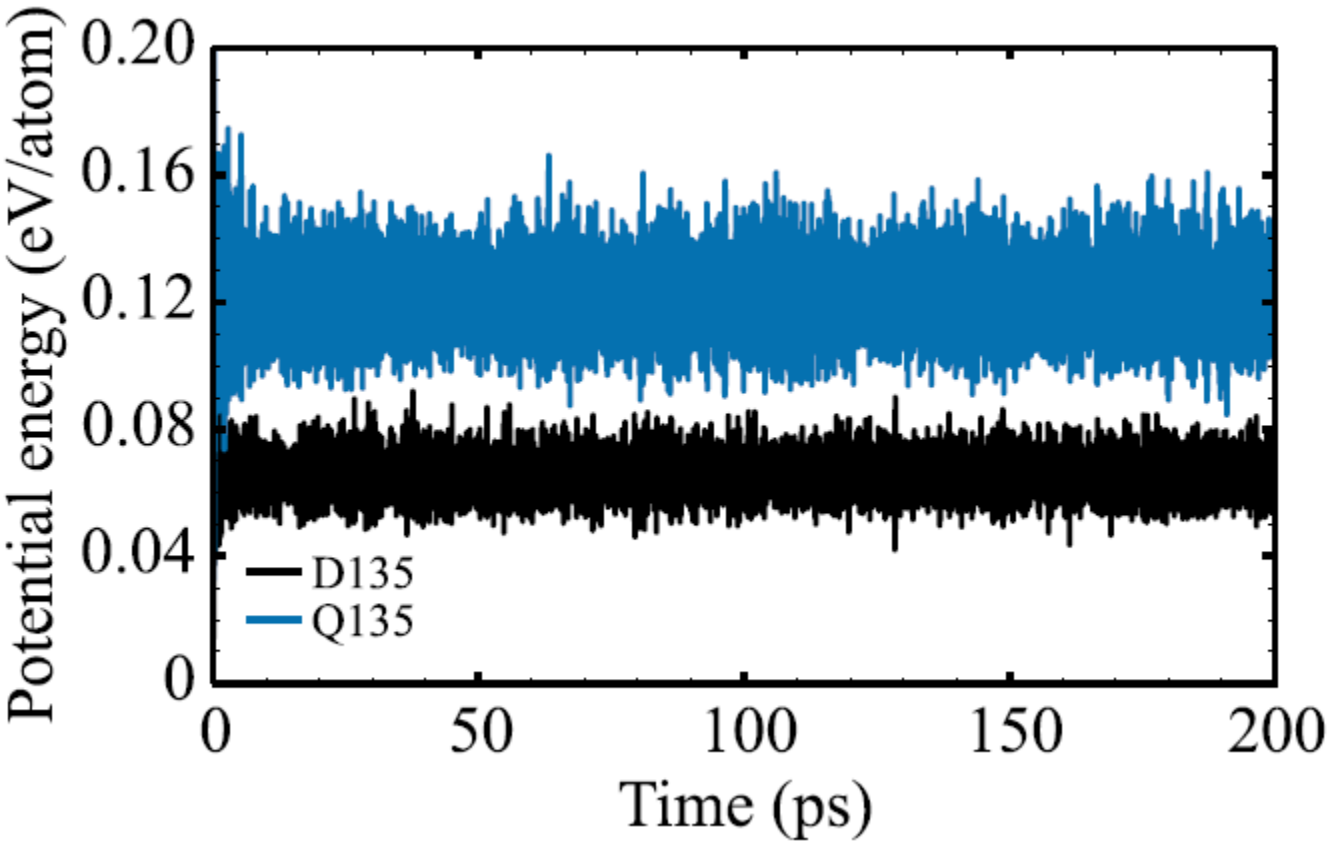

Phys. Rev. B **90**, 115209 (2014).

Imaginary part of dielectric function

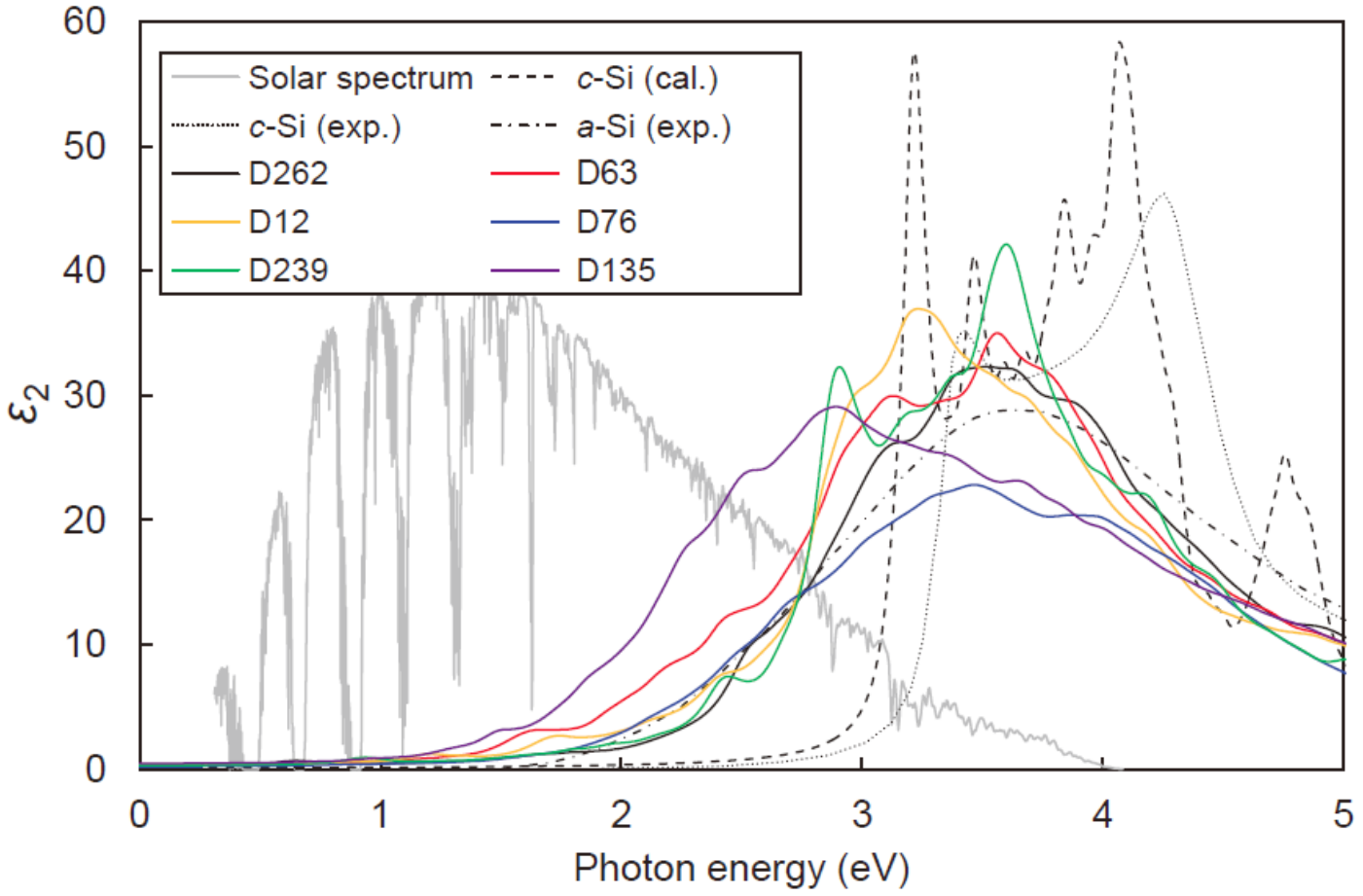

***GW*-BSE**

Phys. Rev. B **90**, 115209 (2014); Comput. Phys. Commun. **203**, 110 (2016).

KRISS

Defects, dipole-allowed, fabrication, toxicity, and cost

Design principle

Selection metric

Being direct does not guarantee good absorption

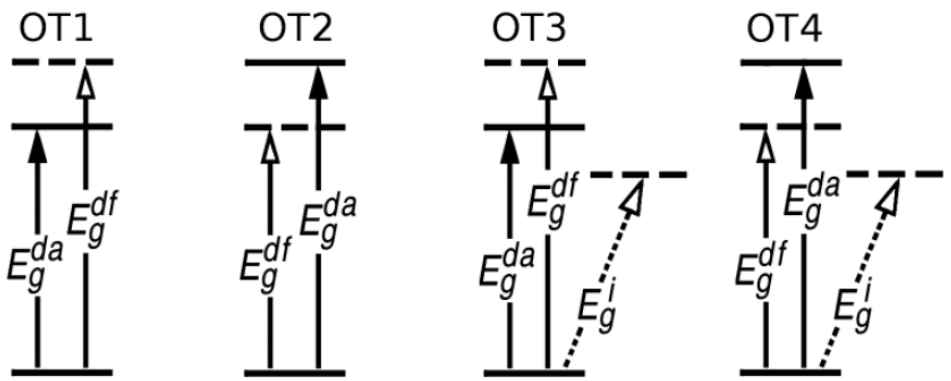

Phys. Rev. Lett. **108**, 068701 (2012).

KRISS

Solar-cell efficiency

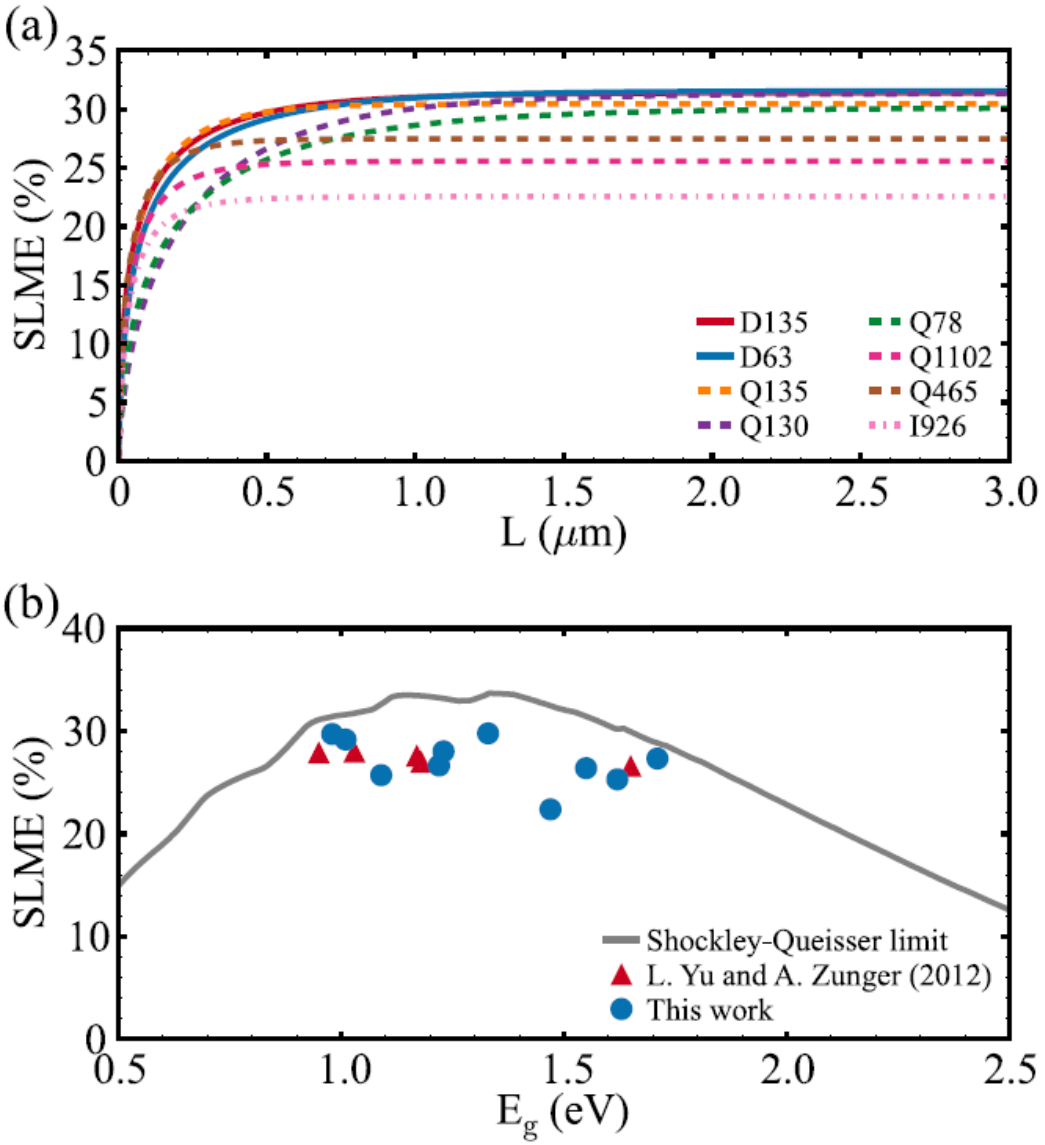

***GW*-BSE**

Phys. Rev. B **90**, 115209 (2014).

J. Appl. Phys. **32**, 510 (1961).
Phys. Rev. Lett. **108**, 068701 (2012).

Solar cell specification

Structure	Type	$E_g^d(G_0W_0-\mathrm{BSE})$(eV)	$E_g^{op}(G_0W_0-\mathrm{BSE})$(eV)	f_r	$L(\mu m)$	V_{oc}(V)	V_{max}(V)	SLME(%)
D135	OT1	0.98	0.98	1	0.5	0.75	0.67	29.71
D63	OT1	1.01	1.01	1	0.5	0.78	0.69	29.17
Q130	OT3	1.01	1.01	0.80	0.5	0.78	0.69	26.64
Q135	OT3	1.33	1.33	2.6×10^{-2}	0.5	0.99	0.89	29.77
I926	OT3	1.68	1.68	8.9×10^{-6}	0.5	1.10	1.01	22.37
Q465	OT4	1.69	1.70	6.3×10^{-2}	0.5	1.34	1.24	22.32
Q1102	OT3	1.70	1.70	2.4×10^{-3}	0.5	1.26	1.17	25.29
Q419	OT3	1.64	1.64	2.2×10^{-3}	0.5	1.20	1.10	26.38
Q78	OT3	1.06	1.06	0.18	0.5	0.71	0.63	25.70
Q636	OT3	1.31	1.31	4.5×10^{-3}	0.5	0.92	0.83	28.02

First-principles electronic structure + CSA *GW*-BSE

Estimated solar cell specification

The optical type, the band gap, the fraction of radiative electron-hole recombination current parameter (f_r), the film thickness (L), the open circuit voltage (V_{oc}), the voltage at the maximum power (V_{max}), and the spectroscopic limited maximum efficiency (SLME) are shown.

Phys. Rev. B **90**, 115209 (2014).

0.09 eV/atom, 1.3 eV

- Synthesis of an open-framework allotrope of silicon

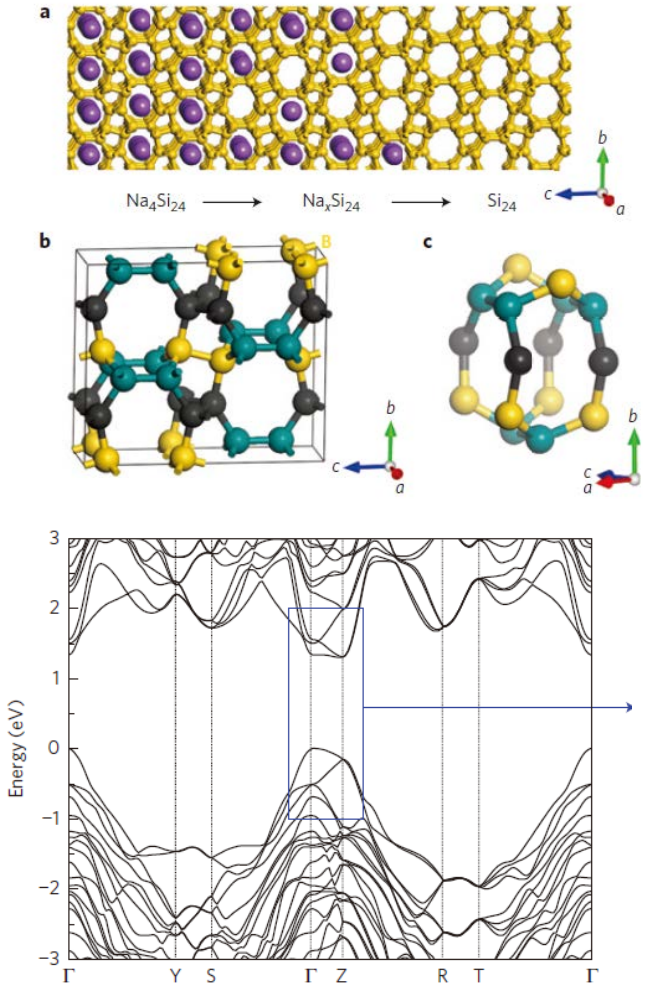

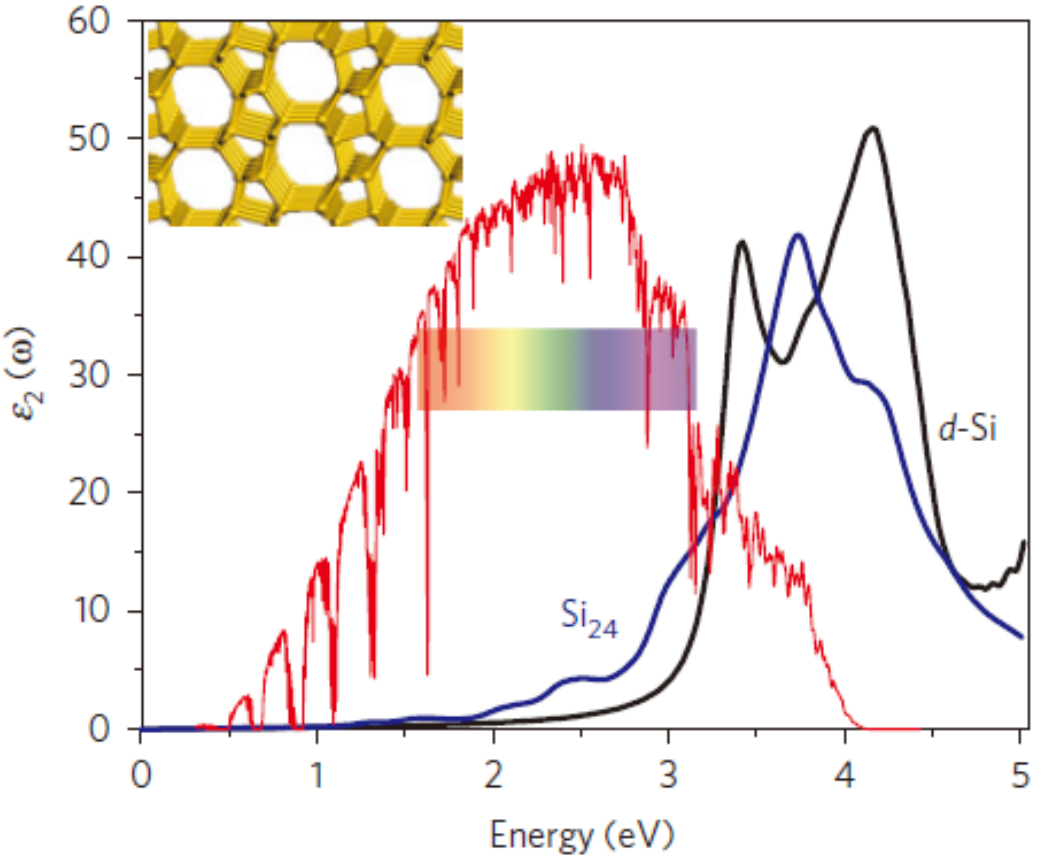

Nature Materials **14**, 169 (2014). PUBLISHED ONLINE: 17 NOVEMBER 2014 | DOI: 10.1038/NMAT4140

Direct band gap silicon superlattices

$Si(111)_{n=3}$/Si(SC) superlattice

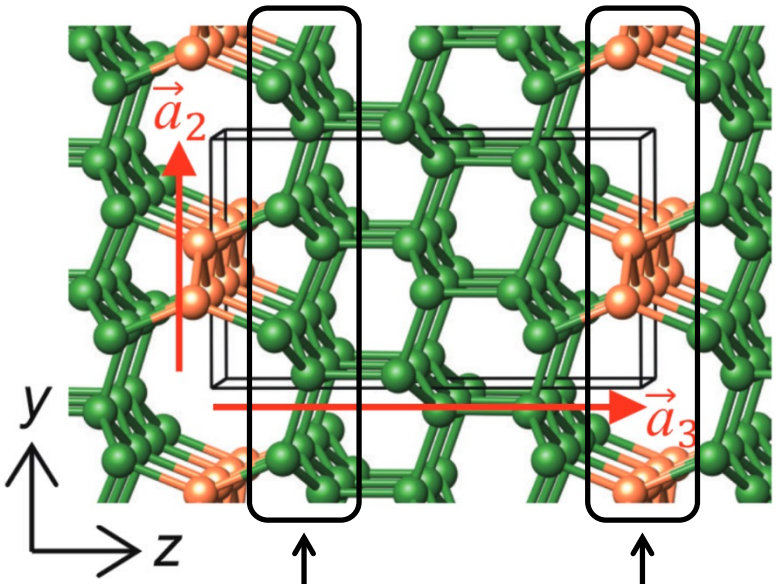

Si(111) layer

Seiwatz chain (SC)

Surf. Sci. **2**, 473 (1964).

PBE eigenvalues

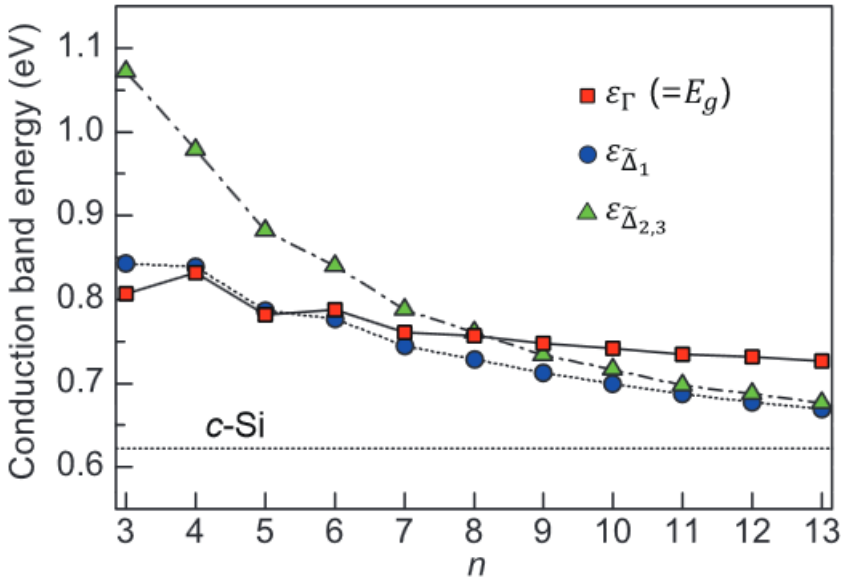

- **direct-to-indirect band gap transition as *n* changes from 5 to 6**

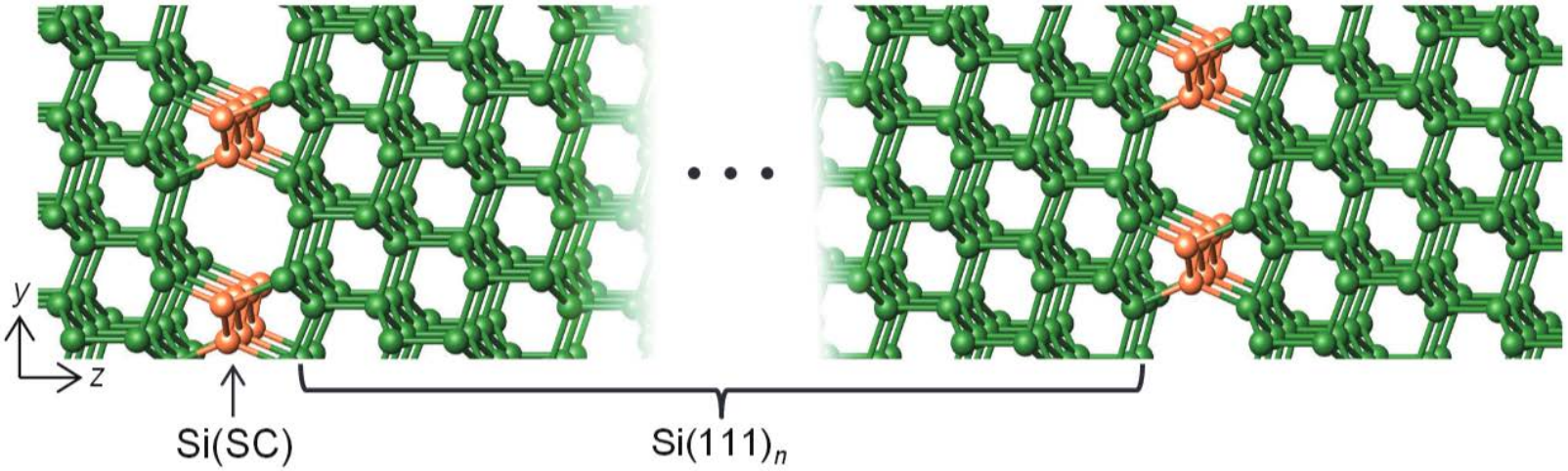

KRISS

Band structure for Si(111)$_{n=5}$/Si(SC)

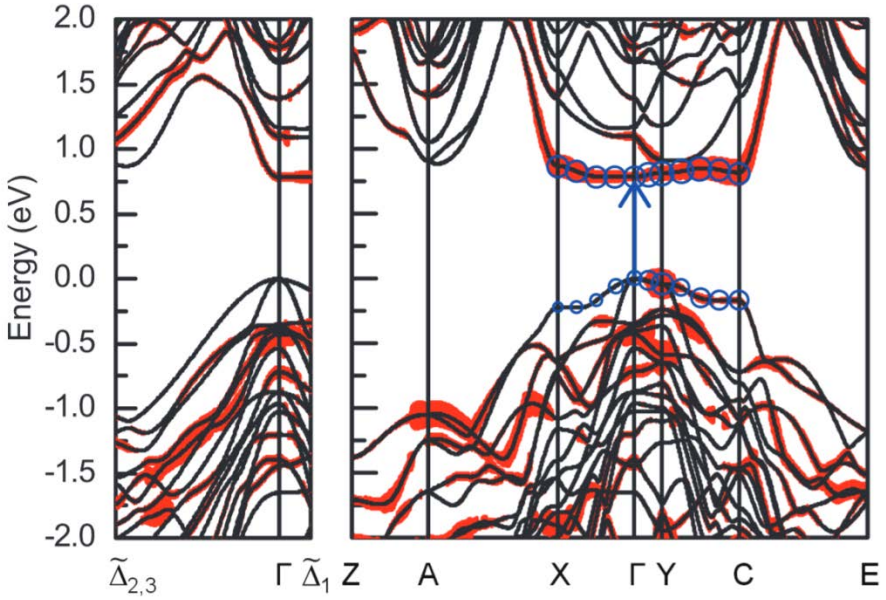

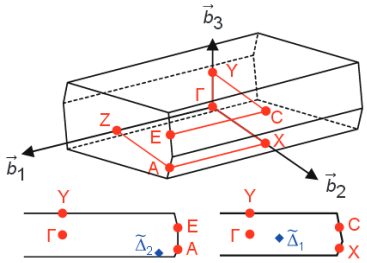

Nearly flat conduction band derived from the defective layer

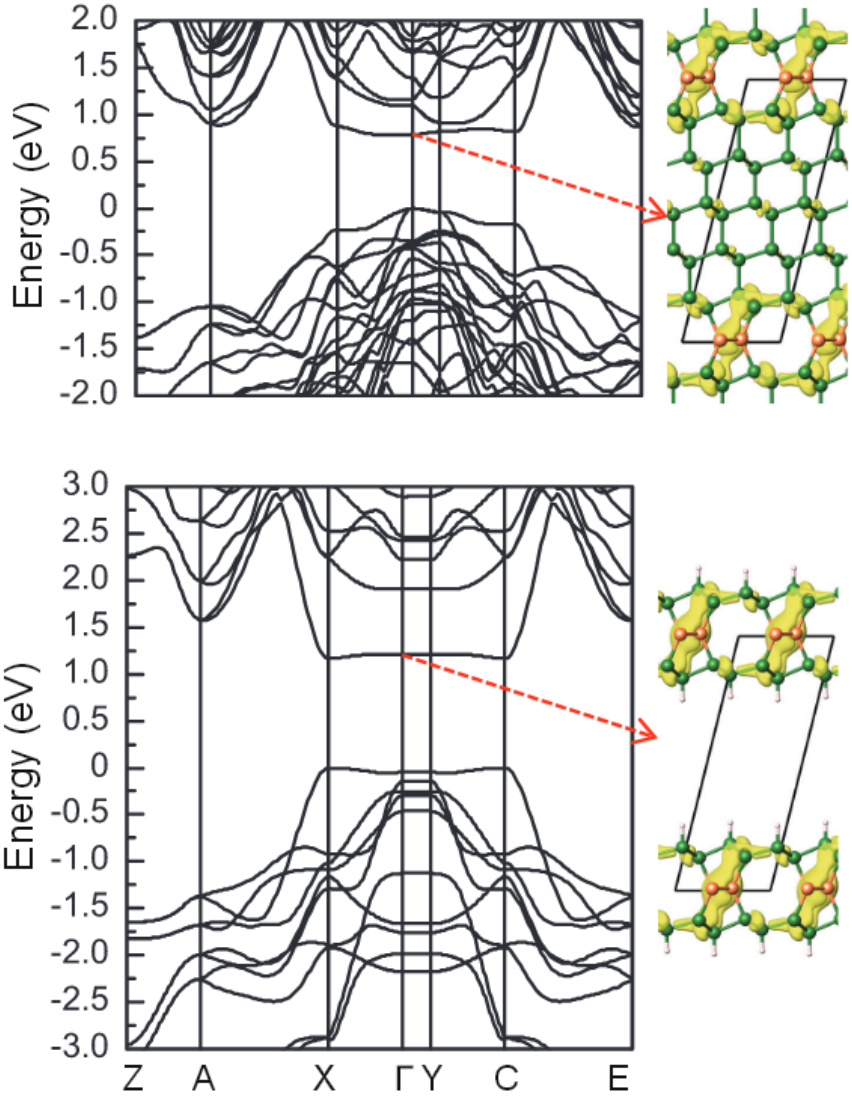

Sci. Rep. **5**, 18086 (2015).

KRISS

Phonon spectra and molecular dynamics simulations

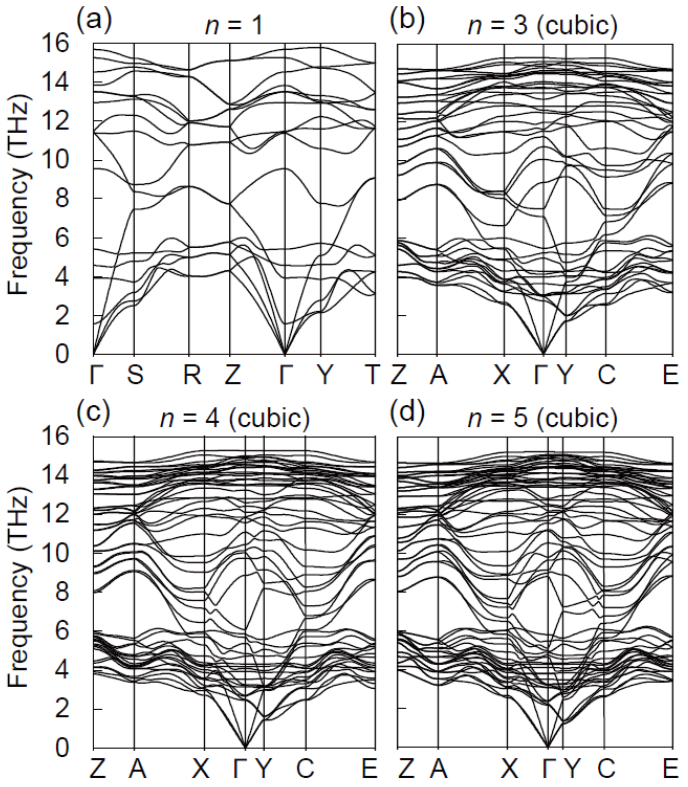

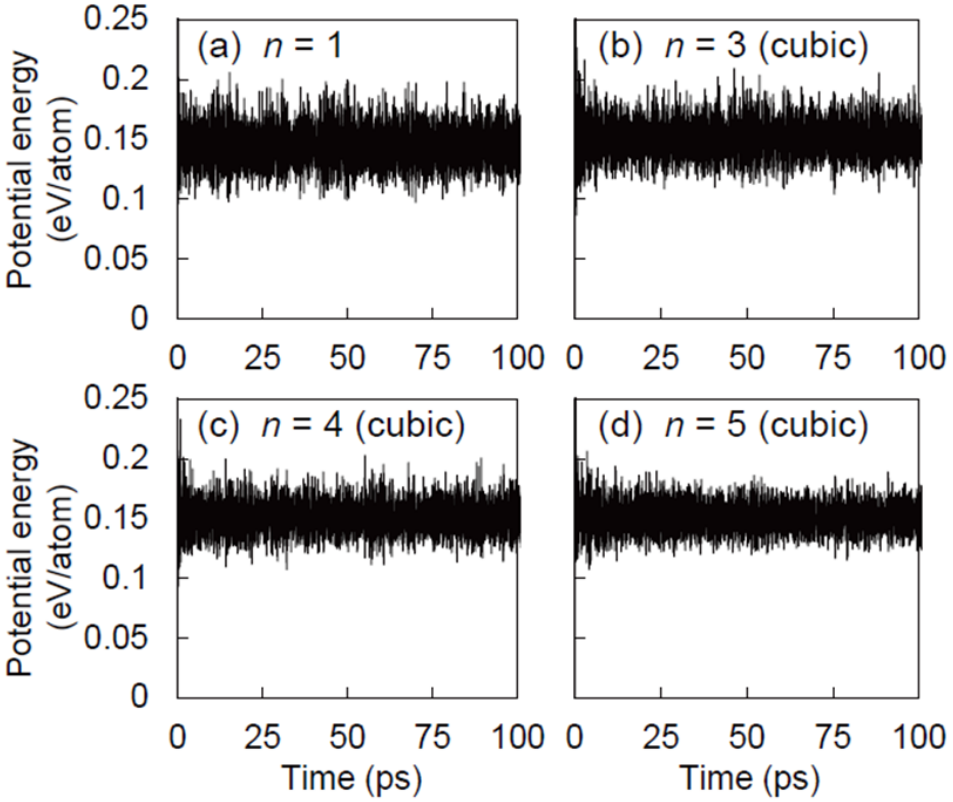

Sci. Rep. **5**, 18086 (2015).

KRISS

Good spatial overlap between VBM and CBM

Band structure for Si(111)$_{n=5}$/Si(SC)

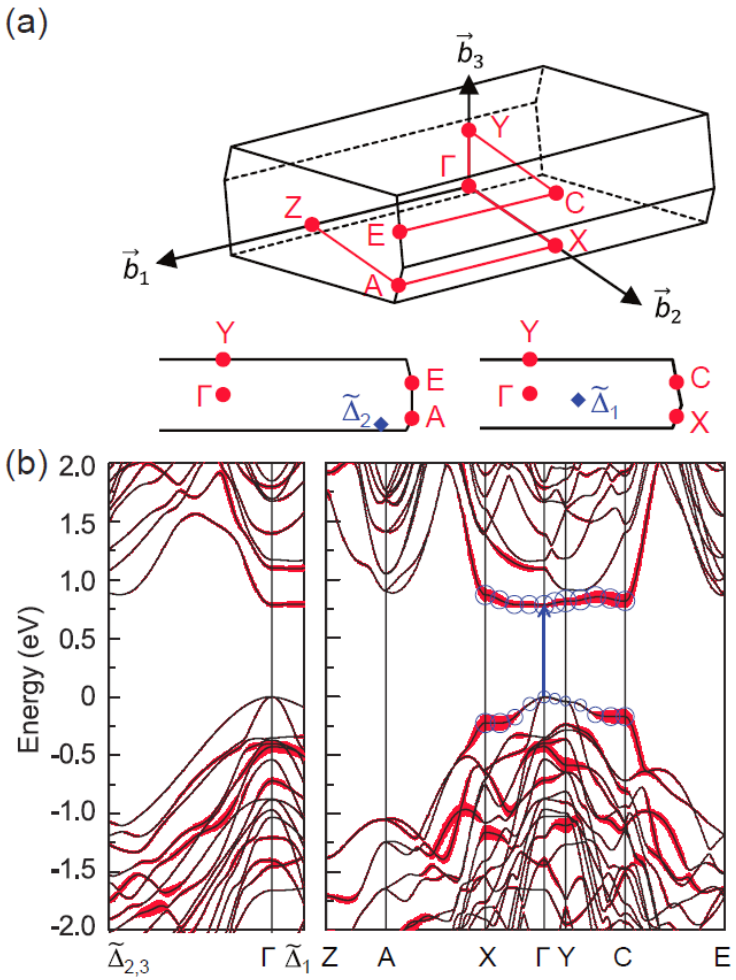

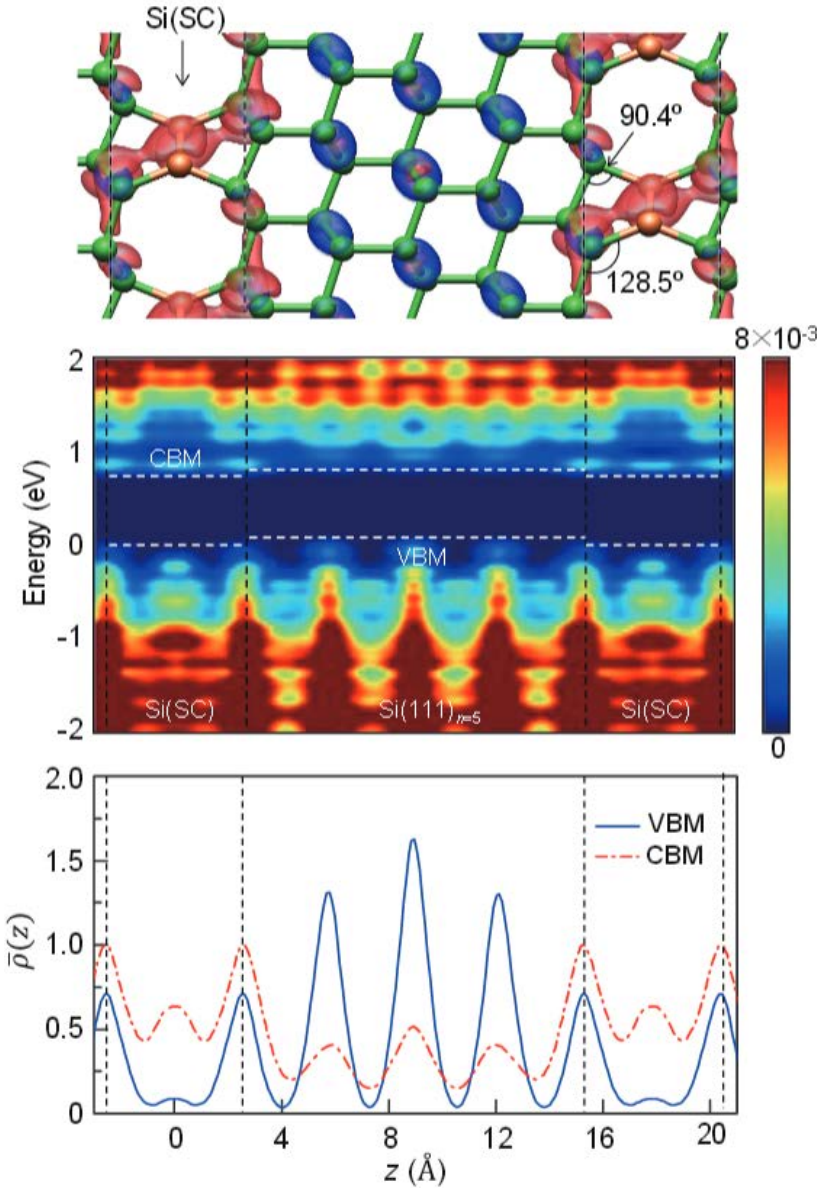

Sci. Rep. **5**, 18086 (2015).

KRISS

Absorption coefficients

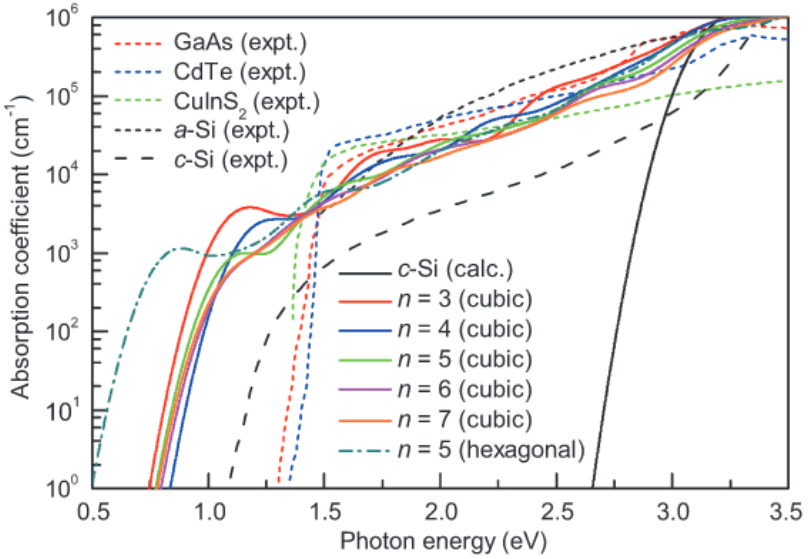

Solar cell efficiency

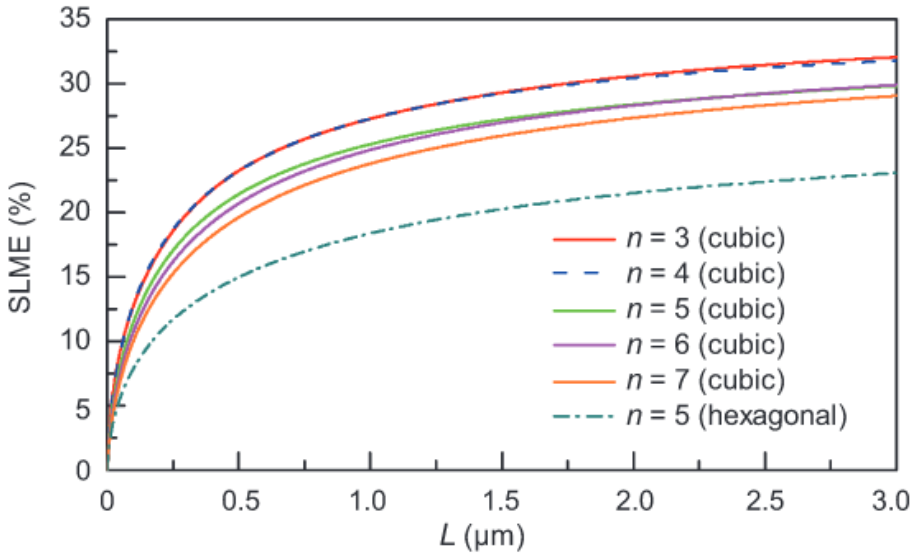

- **The superlattices can be used for thin-film photovoltaic applications.**

Possible synthesis routes

(1) pristine

(2) with half-monolayer of Ca atoms

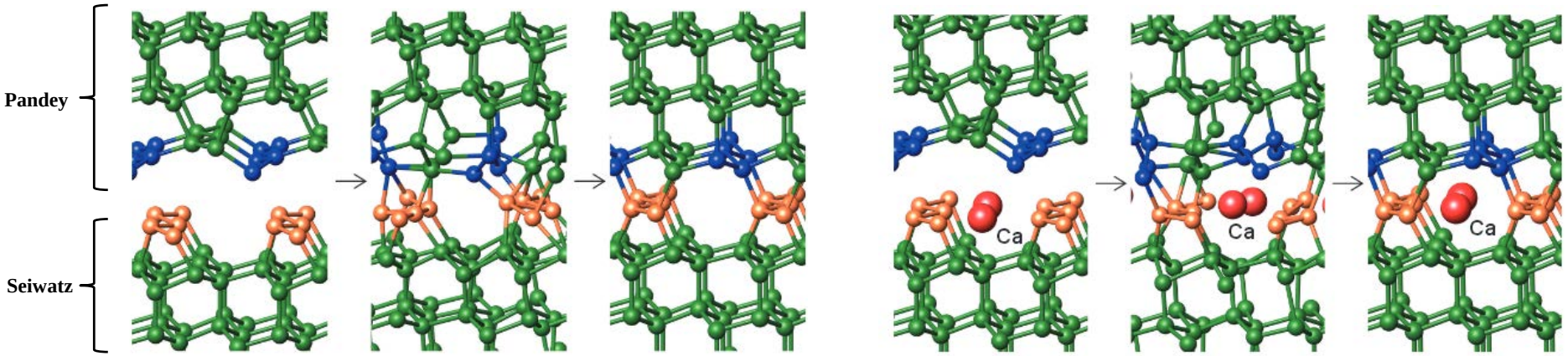

- ***Ab initio* molecular dynamics simulation at 1100 K**
- **Two different Si(111) surfaces: one with Pandey and the other with Seiwatz chain Si(111) 2×1 reconstructed surfaces**

Phys. Rev. Lett. **49**, 223 (1982).
Surf. Sci. **2**, 473 (1964).

Structure, energy, and gap
Dipole-allowed direct-band-gap silicon-superlattices

n	lattice	N	E (meV/atom)	PBE-E_g^d (eV)	PBE-E_g^i (eV)	G_0W_0-E_g^d (eV)	G_0W_0-E_g^i (eV)
1	BCO	6	89 (QD)	0.431	0.430	0.894	0.847
				Cubic-diamond stacking			
2	SM	10	46 (QD)	0.906	0.869	1.346	1.316
3	SM	14	42 (D)	0.807		1.197	
4	SM	18	32 (D)	0.832		1.283	
5	SM	22	26 (D)	0.782		1.218	
6	SM	26	22 (QD)	0.788	0.774	1.224	1.215
7	SM	30	19 (QD)	0.761	0.741	1.198	1.185
8	SM	34	17 (QD)	0.746	0.726	1.185	1.166
9	SM	38	16 (QD)	0.738	0.712	1.177	1.154
10	SM	42	13 (QD)	0.725	0.699	1.167	1.147
				Hexagonal-diamond stacking			
2	SO	10	72 (QD)	0.562	0.527	0.980	0.961
3	SM	14	49 (D)	0.615		1.049	
4	SO	18	30 (D)	0.578		1.008	
5	SM	22	34 (D)	0.497		0.914	

Sci. Rep. **5**, 18086 (2015).

We have predicted several Si crystals with dipole-allowed direct band gaps and good lattice matches with cubic diamond Si, based on a combined approach of CSA algorithm for global optimization and DFT calculations.

Semiconductor Materials		
Material	Chemical Symbol	Bandgap Energy (eV)
Germanium	Ge	0.7
Silicon	Si	1.1
Gallium Arsenide	GaAs	1.4
Silicon Carbide	SiC	3.3
Zinc Oxide	ZnO	3.4
Gallium Nitride	GaN	3.4
Diamond	C	5.5

UV sources

Light comparison			
Name	**Wavelength**	**Frequency (Hz)**	**Photon Energy (eV)**
Gamma ray	less than 0.01 nm	more than 30 EHz	124 keV – 300+ GeV
X-Ray	0.01 nm – 10 nm	30 EHz – 30 PHz	124 eV – 124 keV
Ultraviolet	10 nm – 380 nm	30 PHz – 790 THz	3.3 eV – 124 eV
Visible	380 nm–700 nm	790 THz – 430 THz	1.7 eV – 3.3 eV
Infrared	700 nm – 1 mm	430 THz – 300 GHz	1.24 meV – 1.7 eV
Microwave	1 mm – 1 meter	300 GHz – 300 MHz	1.24 μeV – 1.24 meV
Radio	1 mm – 100,000 km	300 GHz – 3 Hz	12.4 feV – 1.24 meV

- $\lambda < 350$ nm
- AlGaN alloys : deep UV light sources
- GaN-based LED : 365 nm
- AlGaN-based LED, $\lambda < 250$ nm ?

- 5.6 ~ 5.9 eV (210 ~ 221 nm)

https://en.wikipedia.org/wiki/Ultraviolet

KRISS

diamond

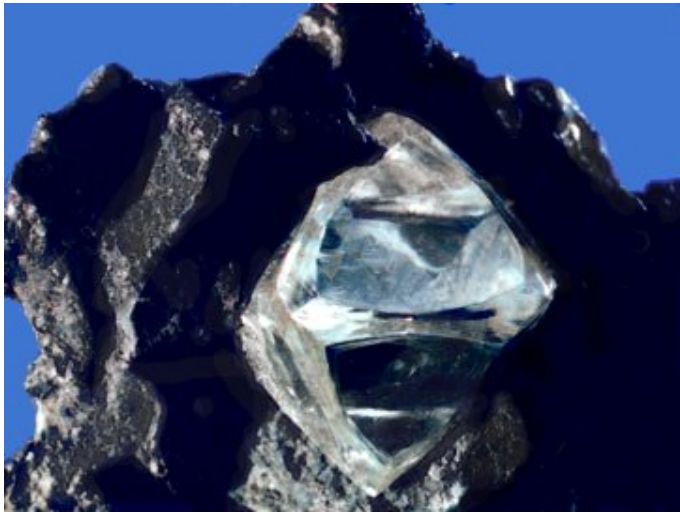

- High electric breakdown field
- High thermal conductivity
- High saturated electron drift velocity
- High carrier mobility
- High thermal stability
- Wide band gap (SiC, GaN)
- Indirect band gap (5.5 eV, 7.1 eV) [G_0W_0; 5.45 eV, 7.34 eV]

- LED; UV curing (photochemical reaction), disinfection
- UV laser: optical sensors, barcodes, DNA sequencing, drug detection, photolithography

Phys. Rev. B **93**, 085201 (2016).

The direct band gaps lie in the range of 5.6 ~ 5.9 eV, corresponding to wavelengths of 210 ~ 221 nm.

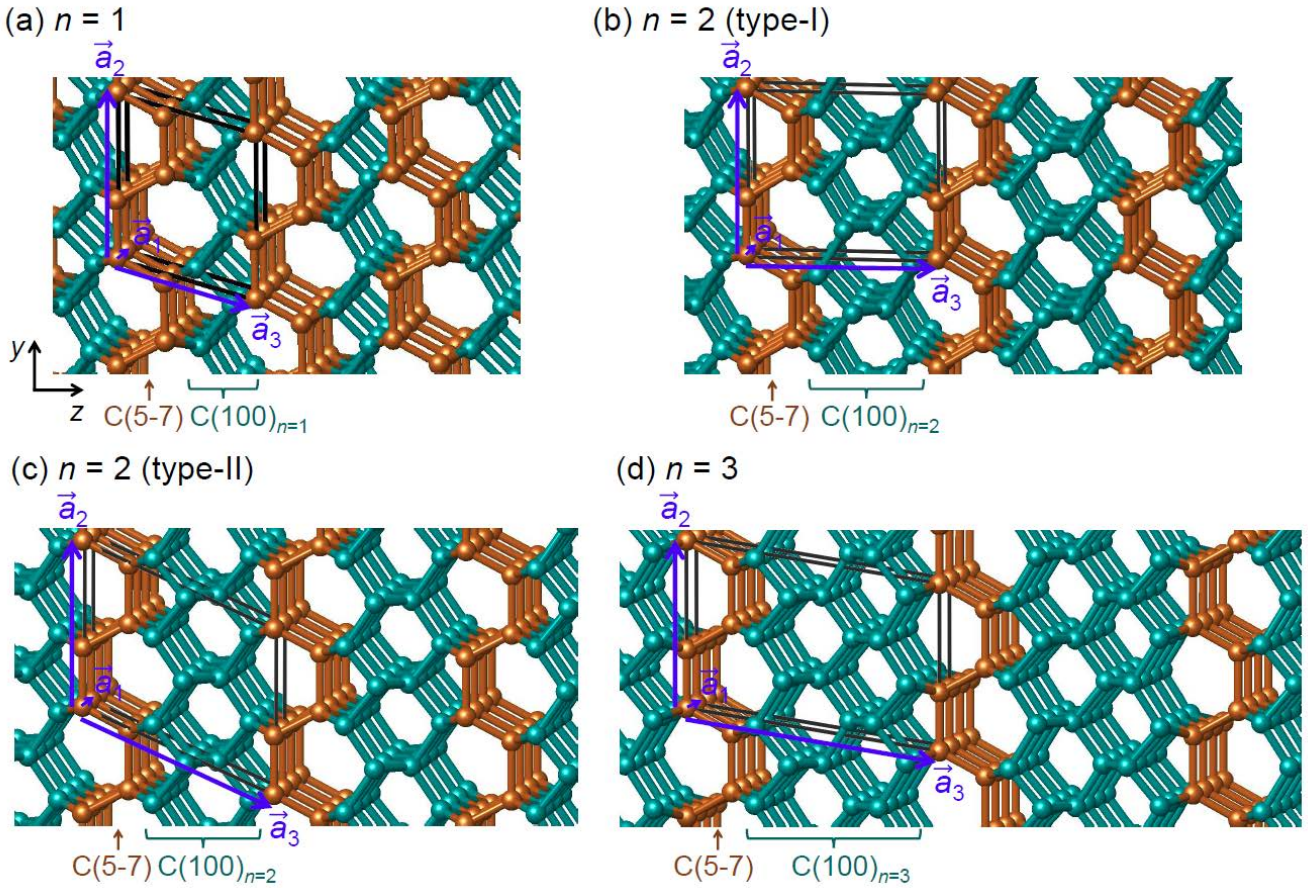

The atomic structures of the $C(100)_n/C(5\text{-}7)$ superlattices for (a) n = 1, (b) n = 2 (type-I), (c) n = 2 (type-II), and (d) n = 3. Colored cyan and brown circles denote the C atoms which belong to the C(100) and C(5-7) layers, respectively. The black parallelepiped represents the unit cell spanned by the lattice vectors, $\mathbf{a}_1$, $\mathbf{a}_2$, and $\mathbf{a}_3$.

Phys. Rev. B **93**, 085201 (2016).

n(type)	N	lattice	Ω_c	E_{tot}	E_g(PBE)	$E_g(G_0W_0)$	space group	previous study
1	8	sm	5.99	164	4.358(ID)	5.550(ID)	$P2/m$ (No. 10)	F carbon [27], J carbon [28]
2(I)	12	base-co	5.88	90	4.311(D)	5.936(D)	$Cmcm$ (No. 63)	S carbon [29], C carbon [30]
2(II)	12	body-co	5.92	134	4.202(D)	5.804(D)	$Imma$ (No. 74)	Z-CACB [31]
3	16	sm	5.85	88	4.163(D)	5.764(D)	$P2/m$ (No. 10)	S-S_1Z_2 [32]
4(I)	20	base-co	5.83	73	4.091(D)	5.679(D)	$Cmcm$ (No. 63)	
4(II)	20	body-co	5.82	70	4.139(D)	5.731(D)	$Imma$ (No. 74)	
5	24	sm	5.81	61	4.076(D)	5.657(D)	$P2/m$ (No. 10)	S-S_1Z_4 [32]
6(I)	28	base-co	5.79	53	4.042(D)	5.614(D)	$Cmcm$ (No. 63)	
6(II)	28	body-co	5.79	53	4.034(D)	5.606(D)	$Imma$ (No. 74)	
7	32	sm	5.78	46	4.001(D)	5.569(D)	$P2/m$ (No. 10)	S-S_1Z_6 [32]

n	space group	a (Å)	b (Å)	c (Å)	β (°)
1	*P2/m* (No. 10)	4.13	2.53	4.78	106.07
2 (I)	*Cmcm* (No. 63)	2.52	11.41	4.91	90.00
2 (II)	*Imma* (No. 74)	2.53	4.87	11.53	90.00
3	*P2/m* (No. 10)	4.93	2.52	7.62	99.32
4 (I)	*Cmcm* (No. 63)	2.52	18.62	4.96	90.00
4 (II)	*Imma* (No. 74)	2.52	4.96	18.60	90.00
5	*P2/m* (No. 10)	4.98	2.52	11.16	96.40

Phys. Rev. B **93**, 085201 (2016).

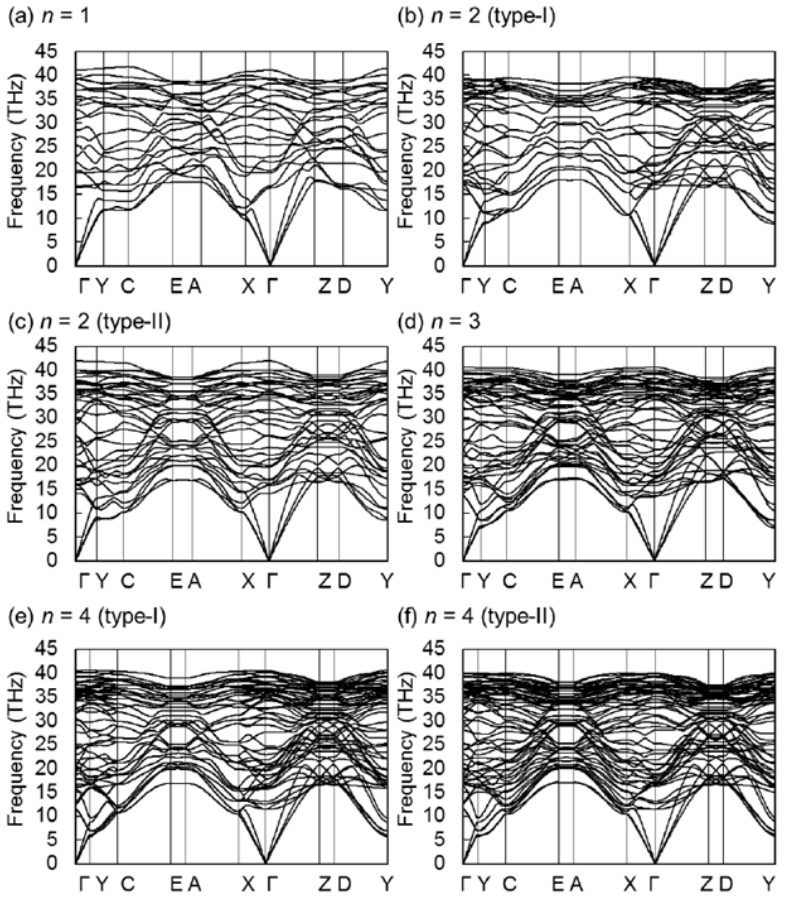

The full phonon spectra of the $C(100)_n/C(5\text{-}7)$ superlattices with n = 1 ~ 4. The dynamical matrices are calculated by using the 4 × 3 × 3, 4 × 3 × 3, 4 × 3 × 2, and 4 × 3 × 2 supercells for n = 1, 2, 3, and 4, respectively.

Phys. Rev. B **93**, 085201 (2016).

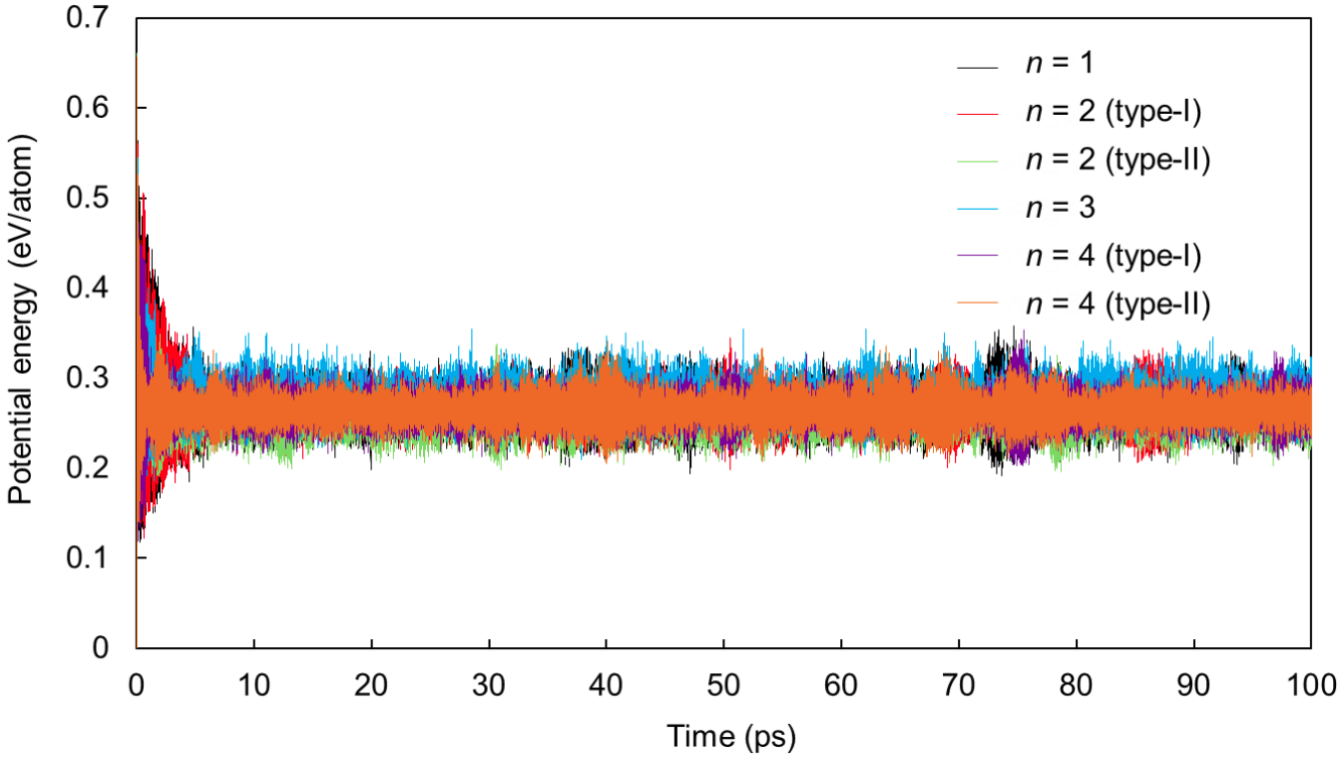

The variations of potential energies during finite-temperature ab initio molecular dynamics simulations at 2000 K are shown for the $C(100)_n/C(5\text{-}7)$ superlattices with n = 1 ~ 4. The 4 × 2 × 3, 4 × 2 × 3, 4 × 2 × 1, and 4 × 2 × 1 supercells are chosen for n = 1, 2, 3, and 4, respectively.

Phys. Rev. B **93**, 085201 (2016).

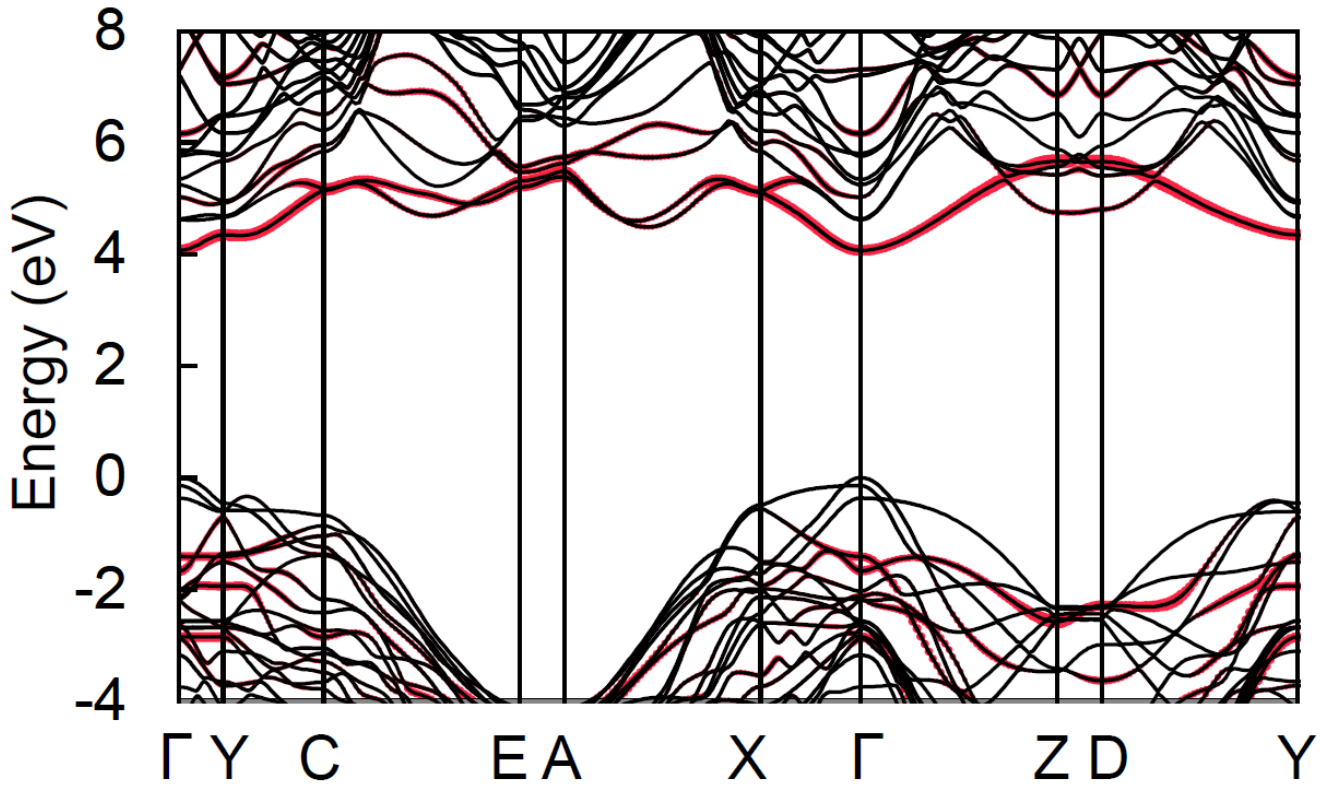

The PBE band structure of the $C(100)_{n=5}/C(5\text{-}7)$ superlattice with the valence band maximum set to zero. The thickness of red colored bands represents the degree of confinement in the defective region.

Phys. Rev. B **93**, 085201 (2016).

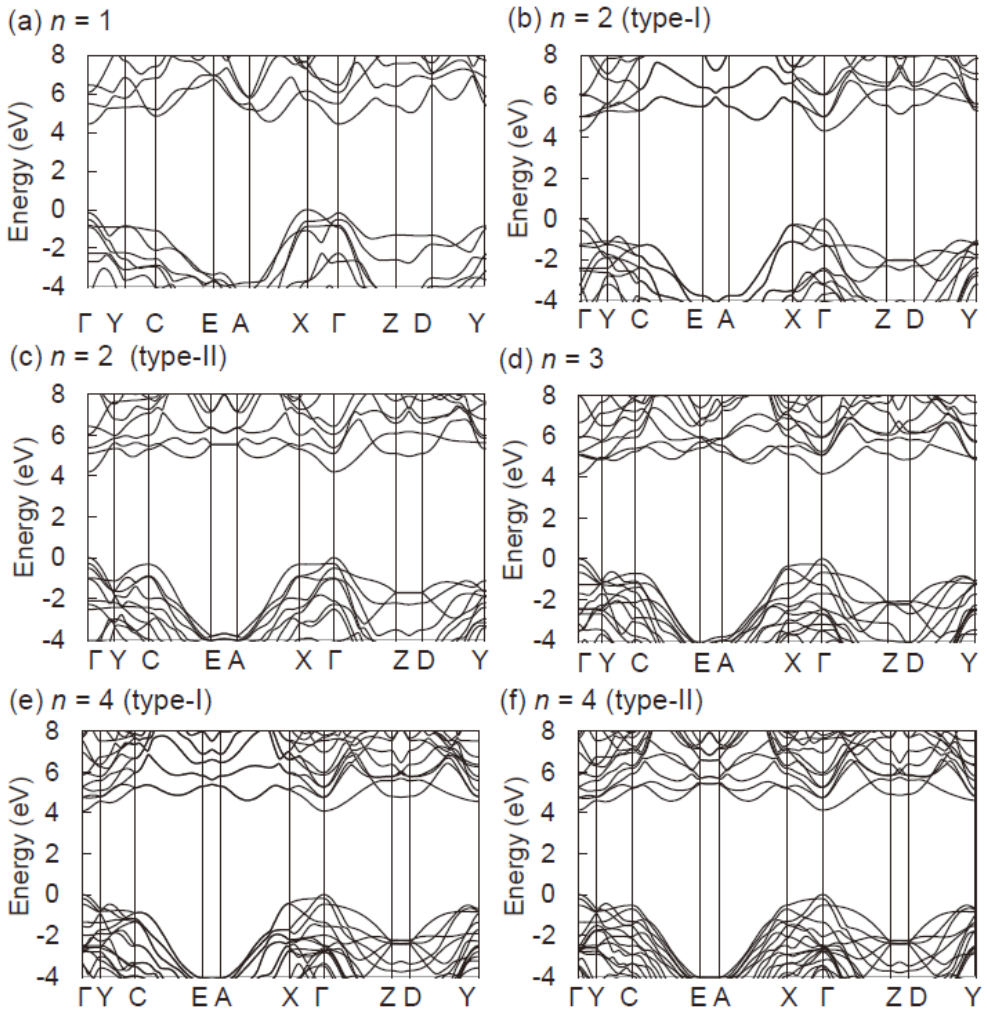

The calculated band structures of the $C(100)_n/C(5\text{-}7)$ superlattices with n = 1 ~ 4 by using the PBE functional. The energy of the valence band maximum is set to zero.

Phys. Rev. B **93**, 085201 (2016).

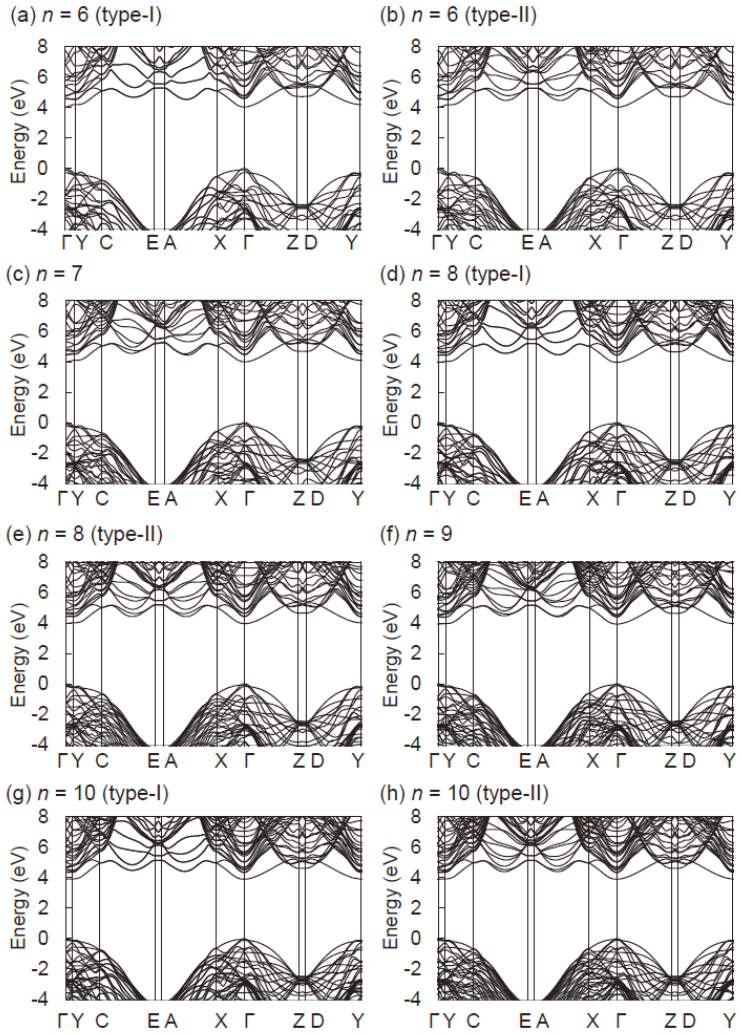

The calculated band structures of the $C(100)_n/C(5\text{-}7)$ superlattices with n = 6 ~ 10 by using the PBE functional. The energy of the valence band maximum is set to zero.

Phys. Rev. B **93**, 085201 (2016).

The dipole matrix elements of direct optical transition are comparable to that of GaN, suggesting that the superlattices are promising materials as an efficient deep ultraviolet light emitter.

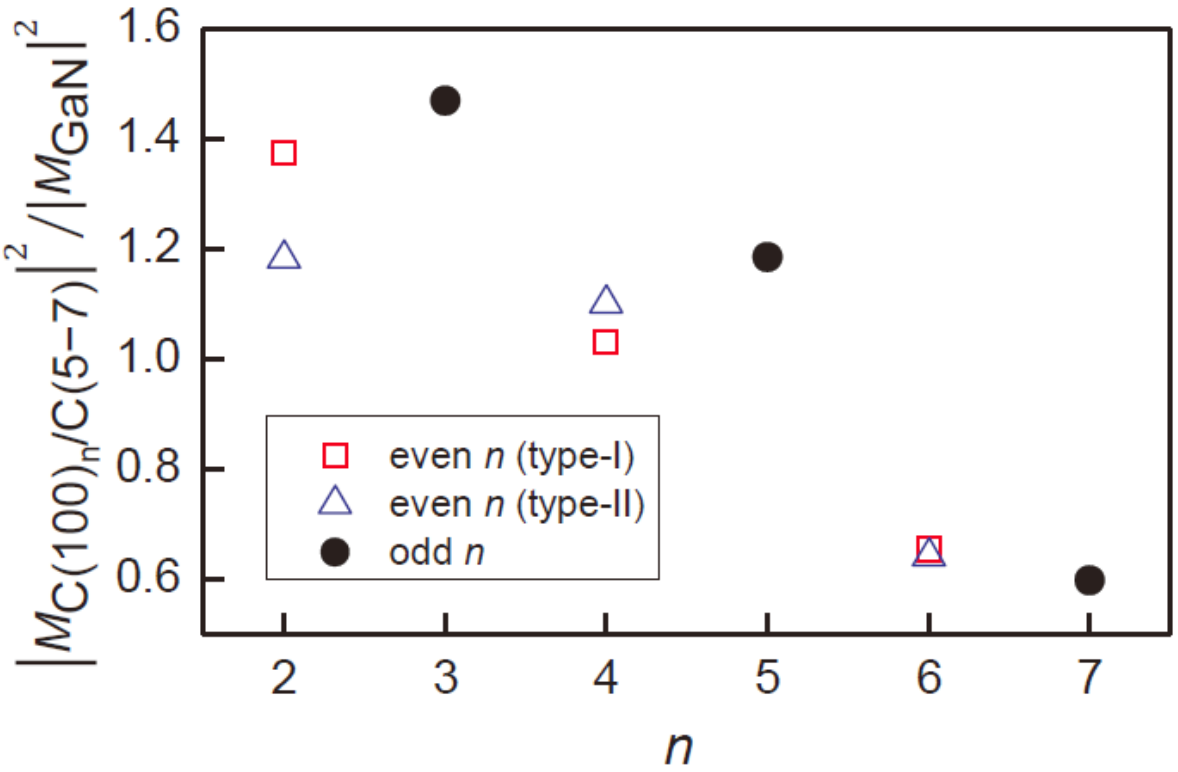

The squares of the dipole matrix elements, $|M_{C(100)n/C(5\text{-}7)}|^2$ for the optical transition at the threshold energy in the $C(100)_n/C(5\text{-}7)$ superlattices are compared with that of GaN, $|M_{GaN}|^2$.

Phys. Rev. B **93**, 085201 (2016).

KRISS

The dipole matrix elements of direct optical transition are comparable to that of GaN, suggesting that the superlattices are promising materials as an efficient deep ultraviolet light emitter.

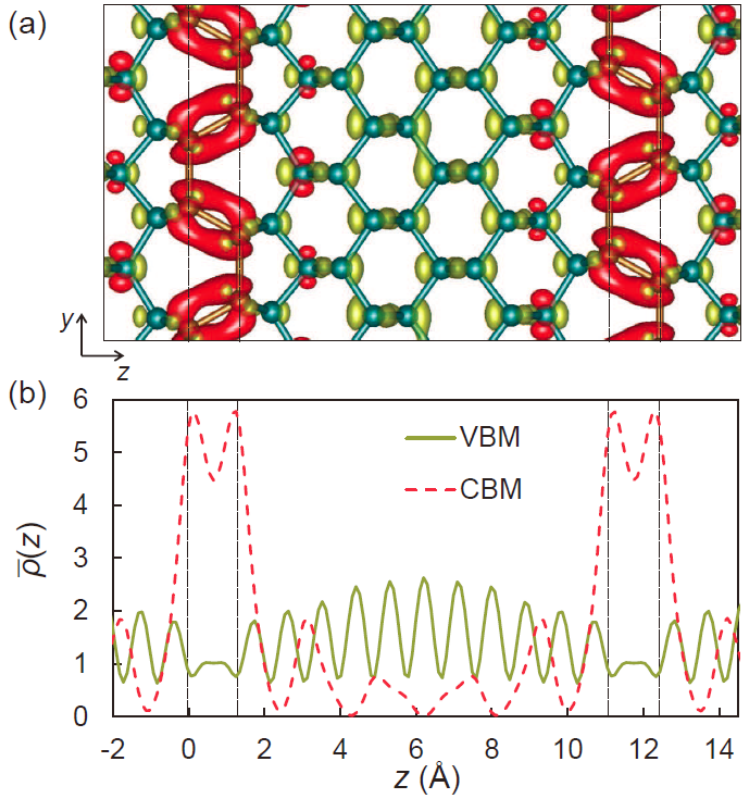

For the $C(100)_{n=5}/C(5\text{-}7)$ superlattice, (a) isosurfaces (0.07 electrons per Å^3) of the charge densities of VBM (yellow) and CBM (red) and (b) their planar-averaged charge densities (in units of 10^{-2} electrons per Å^3) are plotted along the superlattice direction (*z*-axis). Black vertical lines denote the positions of the C atoms in the C(5-7) layers.

Phys. Rev. B **93**, 085201 (2016).

We provide a possible route to the synthesis of superlattices through wafer bonding of diamond (100) surfaces.

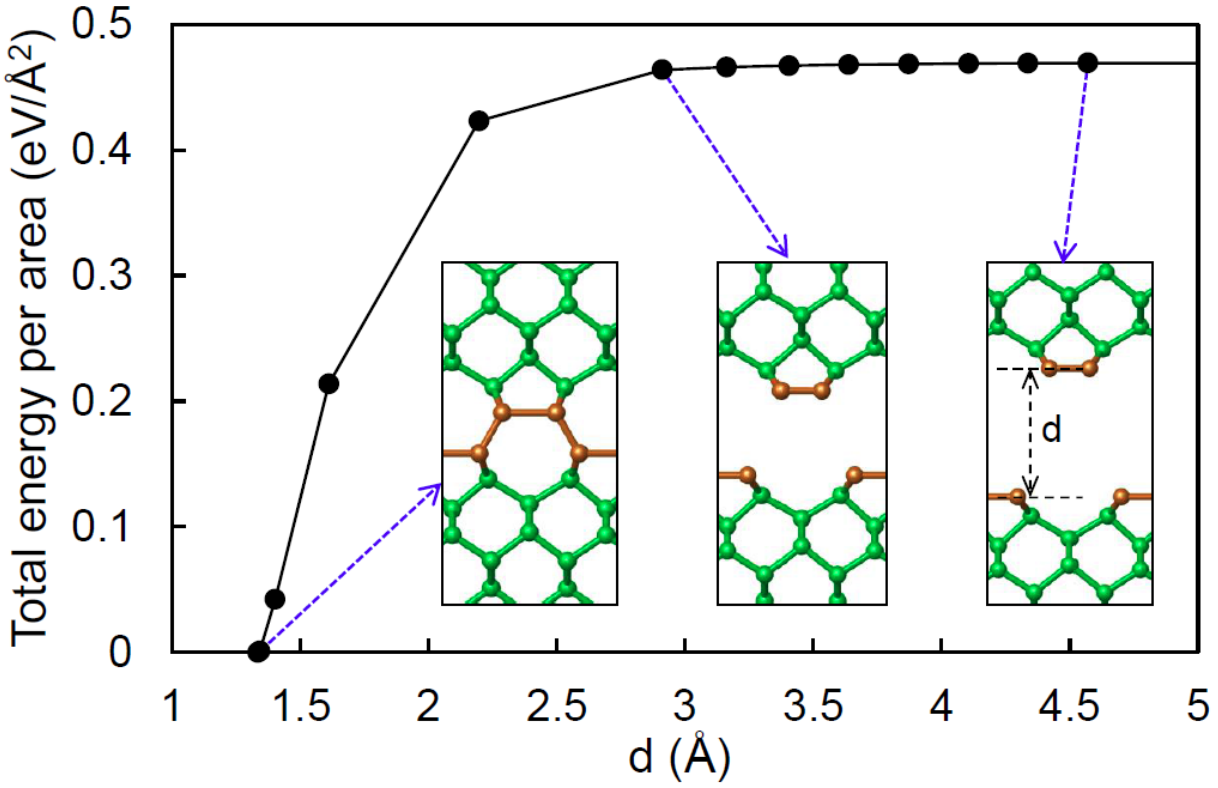

The variation of total energy is plotted as a function of the distance between two clean C(100) surfaces.

Phys. Rev. B **93**, 085201 (2016).

KRISS

Summary

- **We have developed a protocol for computational materials design, called AMADEUS, in which the CSA algorithm for global optimization is combined with first-principles DFT calculations.**

- **We have predicted several Si crystals with dipole-allowed direct band gaps and good lattice matches with cubic diamond Si, based on a combined approach of CSA algorithm for global optimization and DFT calculations.**

- **The optical absorption properties of the designed structures are greatly improved, as compared to *c*-Si, exhibiting excellent photovoltaic efficiencies.**

- **We report pure carbon-based superlattices that exhibit direct band gaps and excellent optical absorption and emission properties at the threshold energy.**

- **The dipole matrix elements of direct optical transition are comparable to that of GaN, suggesting that the superlattices are promising materials as an efficient deep ultraviolet light emitter.**

Phys. Rev. B **90**, 115209 (2014); Sci. Rep. **5**, 18086 (2015); Phys. Rev. B **93**, 085201 (2016); Comput. Phys. Commun. **203**, 110 (2016).